FINAL TECHNICAL REPORT

Paleoseismic Investigation of the Spring Valley Strand of the Bennett Valley Fault,

Santa Rosa, California

Recipient:
Fugro Consultants, Inc. [1]
1777 Botelho Drive, Suite 262
Walnut Creek, California 94596

Infra Terra, Inc. [2]
5 Third Street, Suite 420
San Francisco, California 94103

Principal Investigators:
Janet M. Sowers[1], Jeffrey S. Hoeft[1]
Chris Hitchcock[2], Andrew Barron[2]
Harvey Kelsey[3]

[1]Fugro Consultants, Inc., 1777 Botelho Dr., Suite 262, Walnut Creek, California 94596
Tel: 925-949-7100; email: j.sowers@fugro.com

[2]Infra Terra, Inc., 5 Third St., Suite 420, San Francisco, California 94103
Tel. 925-818-3690; email: chitchcock@infraterra.com

[3]Humboldt State University
Arcata, CA

Program Element:
Element I: Assessing earthquake hazards and reducing losses in urban areas.
U. S. Geological Survey
National Earthquake Hazards Reduction Program
Award Number G15AP00064 / G15AP00065

December 2016

Research supported by the U.S. Geological Survey (USGS), Department of the Interior, under USGS award numbers G15AP00064 / G15AP00065. The views and conclusions contained in this document are those of the authors and should not be interpreted as necessarily representing the official policies, either expressed or implied, of the U.S. Government.

ABSTRACT

The Spring Valley fault is a 5-km-long north-trending fault located on the east side of Santa Rosa, CA, marked by a linear west-facing escarpment, springs, and a linear marsh now occupied by Spring Lake Reservoir. A vertical plane of microseismicity closely aligns with the fault trace. Despite this indirect evidence, the fault is not currently recognized by the State of California as an active fault. Extending between subparallel traces of the Rodgers Creek fault and the Maacama fault, and bounding the eastern margin of the Santa Rosa structural basin, the Spring Valley fault is one of several structures that may play a role in the transfer of slip between these two major faults.

Two trenches at Spring Lake Park, located about 1.6 km (1 mi.) apart, were excavated to accurately locate the fault and to assess the timing of activity. The north trench was sited across a faulted Late Pleistocene terrace remnant of Santa Rosa Creek. This trench exposed gently down-warped fluvial terrace deposits on the east, faulted against colluvium on the west. The fault zone is characterized by multiple sub-vertical seams of clay. Apparent displacement is down-to-the-west, with unknown lateral displacement. The lack of matching units on either side of the fault zone precludes measurement of vertical displacement, but fluvial deposits are absent on the downthrown side to the bottom of the trench at 3 m (9 ft.), suggesting the vertical displacement is significant.

Detailed logging of faulted and down-dropped colluvial wedges west of the fault permits the interpretation of three to five faulting events. Six samples were collected for radiocarbon analysis from the various colluvial units. Of these, three results were used to constrain the event chronology. These were sample 2, from colluvium on the downthrown side of the fault, 2210 to 2310 CAL yr. BP (2 sigma), sample 4, from faulted colluvium on the upthrown side of the fault, 7160 to 6890 CAL yr. BP (2 sigma), and sample 5, from colluvium underlying sample 2, 2860 to 3000 CAL yr. BP (2-sigma).

This study establishes the presence of Holocene faulting along the Spring Valley strand of the Bennett Valley fault. The fault is clearly expressed in two trench exposures, FI-T-1 and SCWA-T1, and is observed to dip steeply to the west. Late Pleistocene fluvial units and Holocene colluvial units are truncated or displaced against the fault. Fluvial units are monoclinally folded on the hanging wall of the fault.

Table of Contents

LIST OF TABLES

LIST OF FIGURES

LIST OF PLATES

LIST OF APPENDICES

1.0 INTRODUCTION

The Spring Valley strand of the Bennett Valley fault may play a role in accommodating ongoing plate-motion in the northern San Francisco Bay region. The Spring Valley strand is the most prominent structure associated with microseismicity that appears to connect the Rodgers Creek fault and the Maacama fault, two major active strike-slip faults (McLaughlin and others, 2008, Hecker and others, 2006, Sowers and others, 2010) (Figures 1 and 2). McLaughlin and others (2008) have proposed that the Spring Valley strand bounds the eastern margin of a pull-apart basin that accommodates a right step between the two major faults. The Spring Valley strand forms a linear 1.6-km long north-south oriented escarpment, west side down, through Spring Lake County Park in the City of Santa Rosa. Our mapping shows that the fault strand exhibits youthful fault-related geomorphic features (Sowers and others, 2010) (Figure 3). The fault, however, is not currently zoned as an active fault by the California Geological Survey (CGS). This investigation builds on our previous NEHRP-funded mapping of the southern Maacama fault and the stepover from the Rodgers Creek fault (Sowers and others, 2010), and helps characterize seismic hazards in the rapidly growing Santa Rosa metropolitan area.

In the study area, the Spring Valley strand forms a 1.6-km long linear north-south striking, west-facing escarpment that extends through Spring Lake County Park. Historical maps and aerial photography document an elongated marsh and springs at the base of the escarpment (Figure 3). The fault bounds an elongate north-north-east alluvial ridge, now partially covered by Spring Valley Dam. Geomorphic expression of the fault weakens to the north and south, but is sufficient for a total mapped length of about 4 km (Sowers and others, 2010).

The preservation of parts of the natural landscape of Spring Valley as a public park provided the opportunity to conduct a paleoseismic study across relatively undisturbed faulted geomorphic features. Interpretation of LiDAR data collected by the City of Santa Rosa, combined with historic topographic construction maps and geotechnical borings completed for Spring Lake Dam, allowed for relatively precise location of the surface expression of the Spring Lake strand.

Although no historical rupture is documented on the Bennett Valley fault, seismicity patterns suggest activity at depth, especially along the Spring Valley strand. Waldhauser and Schaff (2008, updated 2016) show a band of microseismicity closely aligned with the strand (Figure 2, purple dots). When viewed in profile the seismicity defines a nearly vertical plane, consistent with the presence of an active fault (Sowers and others, 2010). In addition, analysis of the 1969 $M_{L=}$5.7 Santa Rosa earthquake on the Rodgers Creek fault, shows a M_L=3.4 shock located within 1 kilometer of the Spring Valley strand (Wong and Bott, 1995), suggesting the earthquake may have triggered a response on the Spring Valley strand (Figure 2). The 2014 M 6.0 South Napa earthquake resulted in increased seep and spring activity along the fault trace within the park, but no increase in microseismicity.

New information on the distribution and timing of fault slip between the Rogers Creek and Maacama fault zones has implications for fault segmentation and maximum earthquake magnitudes. Because the Spring Valley strand is not in itself sufficiently long to independently generate surface rupture, any rupture on the strand is assumed to be an extension of rupture on a major fault such as the Bennett Valley, Rodgers Creek, or Maacama faults.

This project responds to the FY2014 Announcement, Element I of the Research Priorities National Earthquake Hazards Reduction Program (NEHRP), which supports research that "*contributes to improvements in the national seismic hazards maps and to assessing earthquake hazards and reducing*

losses in urban areas." The Spring Valley strand is an uncharacterized, potentially active fault located within a major metropolitan area. This project also responds to the priority topic in northern California to "*improve earthquake recurrence and slip history of active faults*".

The USGS-funded research involved excavation and analysis of two fault-normal trenches in Spring Lake County Park. In related work also presented in this report, two additional fault-normal trenches were excavated for a site-specific fault rupture study on Sonoma County Water Agency (SCWA) property north of Spring Lake County Park, funded by SCWA. Results of this additional work are included with the permission of SCWA.

The goals of this study are to determine presence or absence of Holocene offset, to determine the geometry of the encountered fault, to establish recency of fault rupture, and, if possible, to constrain the rupture history, direction of slip, and amount of displacement of the latest rupture event. In turn, the fault activity could help infer/constrain the timing of large, late Holocene earthquakes on the adjacent Rodgers Creek and Maacama faults.

2.0 GEOLOGIC SETTING AND PREVIOUS WORK

The Rodgers Creek and Maacama fault zones are major active right-lateral faults that represent the northern extension of the Hayward-Rodgers Creek fault system. The Working Group on California Earthquake Probabilities (WGCEP, 2003) defined the Hayward-Rodgers Creek fault system as having the greatest probability (27%) of generating an M ≥ 6.7 earthquake within the next 30 years. Research studies indicate a recurrence interval of about 230 years between major earthquakes on this system (Budding et. al, 1991; Schwartz et. al, 1992). A potential scenario considered by the WGCEP involves the entire Rodgers Creek fault rupturing along with the Hayward fault to produce an earthquake as large as M 7.4. These estimated earthquakes (Mw 6.7 to 7.4) would be associated with an average fault offset of 0.5 m (1.5 ft) to 2.2 m (7.2 ft), with a maximum offset between 0.7 m (2.3 ft) and 3.9 m (12.8 ft). The Rogers Creek fault passes directly through downtown Santa Rosa, merging northward with the Healdsburg fault (Figure 1). The 1969 M 5.7 Santa Rosa earthquake sequence (Wong and Bott, 1995) occurred on the Rodgers Creek fault immediately north of downtown Santa Rosa.

A Quaternary fault map compilation by the USGS and CGS (2009) is shown in Figure 1. Consistent with new LiDAR based mapping by Sowers and others (2009) on the southern Maacama fault, and by Hecker (2010) on the Rodgers Creek fault, the Holocene strands of the two faults overlap for about ten kilometers in the mountains north of Santa Rosa. However, less active strands of these two faults and the Bennett Valley fault overlap for several tens of kilometers. Bedrock mapping by McLaughlin et al. (2004a, 2008) extends the Maacama fault, as a bedrock feature, south across the Mark West Springs quadrangle into Rincon Valley in the Santa Rosa quadrangle.

McLaughlin and others (2004b, 2008, 2012) proposed that the Rodgers Creek fault makes a right stepover to the Maacama fault across Rincon Valley, where the two faults are separated by about five kilometers (Figure 1). Extension within the stepover is thought to have created the Santa Rosa pull-apart basin, which manifests geomorphically as two large valleys – Rincon Valley and Bennett Valley (Hecker and others, 2006) (Figure 2).

Despite an appealingly simple model of extensional stepover creating the Santa Rosa pull-apart basin, the nature of the transfer of dextral slip within the stepover area is not well understood. Our recent study of the stepover supports a model in which distributed slip between the two faults may occur as far north as Healdsburg (Sowers and others, 2010). However, slip on discrete faults may also play an important

role, especially along known bedrock faults such as those mapped by McLaughlin and others (2004a, 2004b, 2008). One of these, the Spring Valley strand of the Bennett Valley fault, is considered to have Pleistocene activity (McLaughlin and others, 2008). The Spring Valley strand is a north-striking fault that splays off the northwest-striking Bennett Valley fault (Figure 2).

McLaughlin et al. (2008) indicate that the Spring Valley strand may accommodate extensional right-normal oblique slip associated with extension of the Santa Rosa pull-apart basin. They also note that the regional distribution of seismicity (Waldhauser and Ellsworth, 2000) further suggests that the Bennett Valley Fault Zone and associated unnamed faults southeast of the map area are associated with northeastward partitioning of slip between the Rodgers Creek and the Maacama Fault Zones. McLaughlin et al. (2008) note youthful geomorphic features on an older map:

"The 1954 U.S.G.S. topographic map shows a linear marsh and springs that are aligned with the Spring Valley strand of the Bennett Valley Fault Zone along the east side of Spring Valley The marsh is now covered by the reservoir."

NEHRP-supported mapping by Sowers and others (2010) adds additional evidence that the Spring Valley strand may be active.

3.0 SITE DESCRIPTION AND METHODOLOGY

Within Spring Lake Park, the Spring Valley fault strand forms a linear north-south, west-facing escarpment, 1.6-km long. Historical maps and aerial photography document an elongated marsh and springs at the base of the escarpment (Figure 3). Geomorphic expression of the fault weakens to the north and south (Sowers and others, 2010). 1942 aerial photography shows a clear linear escarpment along the margin of Spring Valley, a break-in-slope across the alluvial terraces of Santa Rosa Creek, and a topographic lineament extending northward toward the Maacama fault (Figures 3 and 4). A pre-construction topographic map of the Spring Lake reservoir dam site obtained from the Sonoma County Water Agency and historic pre-construction photographs clearly show linear escarpments cutting across late-Quaternary fluvial terraces and a prominent linear ridge within alluvium in the center of the valley further supporting late-Quaternary activity for this fault (Figure 5). Additional geomorphic evidence for young faulting includes springs along mapped fault features and numerous topographic and vegetative lineaments in Quaternary landforms.

The study site lies within the boundary of Spring Lake County Park, which is operated by Sonoma County Regional Parks on land owned by the Sonoma County Water Agency. Trenching activities were coordinated with and approved by both agencies. Trenching procedures followed Cal-OSHA standards, and were conducted under Fugro's CAL OSHA trenching permit.

3.1 Trench Locations

Excavations at Spring Lake Park consisted of two fault perpendicular trenches located approximately one mile apart, near the north and south extremes of the park (Figure 6). The northern trench was positioned across the margin of a faulted alluvial terrace near the main dam, and the southern trench was located across an apparent fault scarp in colluvium at the base of a hillslope south of the reservoir.

The north trench site is located across a preserved north-south striking, west-facing scarp that juxtaposes a fluvial terrace against the sag pond associated with Spring Lake (Figures 6 and 7). As seen on Figure 7, the linear scarp coincides with the truncated western margin of the terrace as identified

in geotechnical borehole transects. Based on observations during the 1962 construction of the emergency spillway near the proposed trench site, the terrace deposits consist of 5 to 10 feet of coarse gravels overlying 'sheared clays' (Figure 5).

The south trench site is located at the mouth of a small gulch south of the lake near the Oak Knolls Picnic Area (Figures 6 and 8). The ephemeral stream in the gulch has built a small debris fan that mantles the fault. Two parallel scarps, mapped from the LiDAR imagery, traverse the colluvial apron adjacent to the fan, and one is expressed in the surface of the fan itself (Figure 8).

Two additional exploratory trenches were excavated across the northwestern mapped trace of the fault, north of Spring Lake Park between Montgomery Drive and the north dam (Figure 6). The trenching was conducted to document the presence or absence of faulting through the footprint of the Sonoma Booster Station for the Sonoma County Water Agency. Trench SCWA-T-1 was located in the parking area northeast of the Booster Station, and consisted of an excavation approximately 50-feet-long and 9 feet deep. Trench SCWA-T-2 was located in the open field north of the station, and consisted of an excavation 75-feet-long and 9-feet-deep. The trenches were separated by approximately 30 feet.

A subtle northwest-facing scarp trending N26°W coincides with the fault exposed in Trench SCWA-T-1. This scarp, although modified by dam construction, is visible in the field and on the 1962 site map (Figure 5). Projection of the fault trace coincides with a pronounced bend in Santa Rosa Creek. No streambank exposures of the fault were observed during a walk along the stream channel conducted for this project.

3.2 Trenching and Logging Methodology

Excavation and logging of trenches FI-T-1 and FI-T-2 within the park were performed over a three-week period in October and November of 2015. The two SCWA-funded trenches (SCWA-T-1 and SCWA-T-2) were excavated and logged in March of 2016.

The trenches were excavated to depths of 2 to 3.5 meters using a backhoe fitted with a 36-inch-wide bucket. Following excavation, the southern wall of each trench was cleaned using hand picks and scrapers. Portions of the northern walls were cleaned as needed to clarify or corroborate stratigraphic relationships. A one-meter grid was established on the cleaned walls using string, a survey tape and bubble level. One-meter grid intersections were marked with a nail and labeled with the grid coordinates on white tape. Each gridded wall was photographed using a digital camera to obtain multiple overlapping images.

In the office, the photographs were downloaded and AGISOFT photogrammetry software was used to produce a 'seamless' rectified image of the trench wall exposure. Scaled panels of each image were taped to boards and fitted with mylar overlays. Meanwhile, field geologists interpreted and marked stratigraphic contacts, faults, and other features using nails and colored flagging-tape on the wall of each trench. Once complete, the geologic interpretation was drawn in pencil on the mylar overlays by field geologists, using the seamless photograph as a base-image.

4.0 PALEOSEISMIC TRENCH RESULTS

Results show clear evidence of faulting coincident with mapped fault traces in two of the four trench exposures. The subsections below describe the major stratigraphic and structural geologic features revealed in each trench exposure. The text is accompanied by detailed photographic and geologic logs. Logs of the two NEHRP-funded trenches are presented in Plates 1 and 2, and the log of one SCWA-

funded trench is presented in Plate 3. An enlargement of the log of the fault zone in trench FI-T-1 is presented in Figure 9.

4.1 Stratigraphy and Structure of Trench FI-T-1

The northern trench, FI-T-1, located across the west facing margin of a fluvial terrace (Figure 7), was 36 meters long and 2.5 to 3 meters deep. The fault zone was identified at approximately Station 27 (Plate 1, Figure 9), near its mapped location at the base of the terrace riser. The fault truncates the fluvial terrace deposits on the east side, and juxtaposes them against colluvial deposits on the west side. No fluvial terrace deposits were identified on the west side of the fault zone within the 3-meter deep exposure. Complete unit descriptions are provided in Table 1, and presented on the trench log (Plate 1).

4.1.1 Trench FI-T-1 Stratigraphy

The stratigraphy on the east side of the fault zone consists of stratified sandy, silty and gravelly alluvial deposits overlain by colluvium and artificial fill. The alluvial deposits were deposited by Santa Rosa Creek, and were derived from the Pliocene Sonoma volcanics, and Cretaceous Franciscan melange and serpentinite that underlie the watershed (Wagner and Bortugno, 1982). Clast lithologies identified in the gravel component of the alluvium include basalt, clastic sedimentary rocks, quartz, chert, and volcanic lithics. The alluvial deposit includes logged units 300, 400, 425, 450, 500 and 600 (Plate 1 and Figure 9).

Unit 600, the lowest and oldest unit, consists of massive gravelly clay with some mappable beds of gravel and sand. The overlying two units, 500 and 405, are interpreted to be soil horizons developed on this deposit (Appendix A). Unit 500, a Btq horizon, is a clay to sandy clay, with accumulation of clay on ped faces and coatings of a pale brown mineral (silica?) on fracture faces. Unit 400, laterally correlative to unit 405, is interpreted to be colluvium derived from units 500 and 405, and extends downslope to form a blanket over the entire package of alluvial deposits. The dark gray color of the unit 400 colluvium reflects the incorporation of organic matter during A-horizon development.

Unit 425 overlies unit 500 and is exposed from station 21 to 27, where it is downwarped toward the fault zone. This unit is a maximum of 1.4 meters thick, and consists of alternating beds of gravelly, clayey sand, and silt with fine sand. Gravel clasts include volcanics. The lower half-meter of unit 425 features disseminated reddish brown stains of iron oxide.

Unit 425 is truncated at the base of overlying colluvial unit 400, forming an angular unconformity tha post-dates the deformation of unit 425. Colluvial unit 400 is a dark gray clay, interpreted as a buried A horizon.

Fluvial units 450 and 300 occur near the crest of the terrace from stations 3 to 9. They consist of clayey sands with gravel, and are interpreted to be channel fill deposits. These deposits, and probably other alluvial deposits upslope, are the source of colluvial deposit 200, which mantles the entire slope from the top of the terrace to the fault zone. At the fault zone, unit 200 is truncated by the fault and abuts colluvial unit 180, which is likely derived from unit 200 based on their similarity in gravel content and clast size.

Evidence for grading associated with dam construction is the missing A horizon of colluvial deposit 200. Colluvial unit 200 would have included a topsoil layer; this layer may have been removed at the time of dam construction.

The upper-most stratigraphic unit, unit 100, is a disturbed layer that contained anthropogenic debris including broken glass fragments. The fill likely was emplaced during the construction of the Spring Lake dam. The fill forms a mantle 0.4 to 0.7 m thick over the entire trench.

On the west side of the fault zone, the stratigraphy consists of a series of fine-grained colluvial deposits, also overlain by artificial fill. Five main colluvial units, in order from oldest to youngest, are units 250, 240, 180, 160, and 150. All are clayey silts to silty clays with sand and gravel, exhibiting no fluvial stratification. The oldest unit, 250, is highly weathered and cannot be clearly correlated with any unit on the east side of the fault.

Unit 240 is folded or draped over the scarp face and is either continuous with or derived from unit 400 on the east side of the fault. Vertical displacement, measured from the base of unit 240 on the downthrown side to the base of unit 400 on the upthrown side, is 1 to 1.5 meters. West of the fault zone, unit 240 is a horizontal planar bed up to one meter thick.

Unit 180, overlying unit 240, is a coarse gravelly clay that is interpreted to have been derived from coarse gravelly colluvial unit 200, which mantles the hillslope on the east side. The coarse gravels originated from fluvial deposits of Santa Rosa Creek (eg. unit 300), gradually eroded and brought down the hillside as colluvial unit 200, then deposited on the fault scarp as colluvial unit 180. Vertical displacement, measured from the base of unit 180 on the downthrown side to the base of unit 200 on the upthrown side, is 0.5 to 1 meters.

Colluvial units 160 and 150, the youngest of the colluvial units on the downthrown side of the fault, consist of clayey silt with sand and gravel, and cannot be correlated with units on the upthrown side. The correlative units may have been eroded away, or these colluvial units were deposited at the base of the scarp by a source out of the plane of the exposure.

4.1.2 Trench FI-T-1 Fault Zone and Features

The FI-T-1 trench exposure exhibits fault features including truncated beds, clay-filled vertical fractures, and folding of the beds (Plate 1 and Figure 9). Fault strands are mapped primarily on the basis of the truncation or displacement of bedding and the presence of vertical fractures, often lined with clay.

The fault zone consisted of a vertical shear zone 1.5 to 2.0 meters wide displaying apparent down-to-the-west displacement and an unknown amount of lateral displacement. A series of truncated and stratigraphically offset layers were documented within the fault zone. No in-situ, undisturbed layers were observed across the fault zone, with the exception of the overlying historically emplaced artificial fill.

The fault zone is cut by multiple vertical to subvertical clay-filled fractures, a few millimeters to a centimeter wide. The main fault is an anastomosing zone of fractures and of clay gouge a few centimeters thick.

The main strand of the fault, at station 27, dips approximately 80 degrees to the west and is an anastomosing zone of fractures 10 to 20 cm wide, truncating fluvial bedding in units 600 and 425 on the east and juxtaposing these two units against colluvial units 180, 240, and 250 on the west. A zone of clay fault gouge (unit 410) is identified on the west side of the fault near the base of the trench. The fault can be traced upward to define the contact between colluvial unit 400 and colluvial unit 240, the latter interpreted to be derived from unit 400. Together, units 400 and 240 drape the underlying fault scarp.

The alluvial deposits are monoclinally folded in proximity to the fault zone. Fluvial bedding in units 500 and 425 dips approximately 20 degrees to the west from zero to six meters from the fault zone, (stations

21 to 27). Mid-slope, both bedding and buried soil profile horizon boundaries are approximately parallel to the ground surface, dipping 5 to 10 degrees to the west. Further east, the dip of units 500 and 600 decreases up slope to about 2 degrees at the top of the terrace These relationships suggest that the slope of the face of the terrace riser may be a monoclinal fold rather than a product of scarp lay-back by erosional processes. This interpretation is consistent with the lack of dissection features on the face of the terrace riser, and will be discussed further in section 5.

4.2 Stratigraphy and Structure of Trench FI-T-2

The southern trench, FI-T-2, located across the fault trace on a debris fan at the mouth of a small drainage (Figure 8), was 25 meters long and 2.5 to 3 meters deep. No fault zone was identified, and continuity of bedding precludes significant faulting of colluvial deposits that overlie the debris fan (Plate 2). However minor folding is not precluded given the coarse, poorly bedded nature of the deposits. Complete unit descriptions are provided in Table 2, and presented on the trench log (Plate 2).

4.2.1 Trench FI-T-2 Stratigraphy

Trench FI-T-2 exposes colluvium that was deposited on a debris fan at the mouth of a small drainage. This drainage is incised into hills on the upthrown side of the fault. The hills are underlain by Pliocene Sonoma volcanics; colluvium includes angular to subrounded gravel clasts composed of volcanic rock.

Five colluvial units, units 10, 20, 30, 40, and 50 are mapped and described on the south wall of the trench exposure (Plate 2). Most units extend the entire length of the trench exposure. The various units are distinguished on the basis of texture, gravel content, and color (Table 2).

The uppermost deposit, unit 10, is a sandy silt with clay and minor gravel, interpreted as an A-horizon that has been partially reworked by grading based on its variable thickness and mounded appearance at station 12. This mound, which extends in a north-south direction, had been interpreted by the team as a fault scarp in aerial imagery, but based on the planar contacts between underlying units, the mound is more likely to be the result of grading for a road or trail.

Unit 20, is a sandy, silty clay with coarse subrounded to subangular volcanic clasts, poorly graded with no discernible bedding. Based on soil profile development, this unit is similar in age to unit 10 and probably represents an AB horizon developed within the same colluvial depositional unit as unit 10. Weak prismatic structure within

Unit 30 is the most distinct and recognizeable unit in the trench, composed of bedded sandy clay with gravel which are assumed to be watery debris flow deposits. The unit is subdivided into two layers, likely deposited within a short time interval, whose upper and lower contacts can be traced continuously from station 10 to station 19.

Units 40 and 50 together comprise an older colluvial deposit, deeply weathered, that abruptly underlies the colluvium of units 10, 20 and 30. These older deposits are massive sandy silts with minor clay and 50% gravel, with no discernible bedding. A prominent feature of unit 40 between stations 0 and 7 is the occurrence of subvertical fractures filled with 1 to 3 mm of light-colored material. These fractures are absent east of station 7, and may represent dessication cracks, or may have a structural origin as discussed in the following subsection.

4.2.2 Trench FI-T-2 Structural Features

Trench FI-T-2 exhibits no structural features that can be positively linked to faulting or folding. The weak

colluvial bedding is approximately planar with minor undulations, all of which may be attributed to original deposition. Based on mapping from aerial photography and topography, and projection of the hill front across this drainage, the main strand of the fault was predicted to intersect the trench at approximately station 11. However, unit 30, a gravelly unit with planar fluvial bedding, forms a continuous layer from station 10 to station 19. Its presence precludes faulting in this zone (Plate 3).

There is some evidence for gentle folding of units 40 and 50, though the evidence is not conclusive. The top of unit 40 exhibits a gentle convexity near station 5 and concavity near station 10 that may be interpreted as a monoclinal fold. Filled vertical fractures documented in unit 40 west of station 7 may represent extension cracks in the crest of the fold. This type of deformation would be consistent with the down-to-the east monoclinal folding documented in trench FI-T-1.

4.3 Stratigraphy and Structure of Trench SCWA-T1

The northern trench, SCWA-T1, located across a subtle south-west facing scarp in the parking area northeast of the Sonoma Booster Station located north of Spring Valley dam was 15 meters long and 3 meters deep. The fault zone was identified between Stations 5 and 7 (Plate 3), near its inferred location at the base of the scarp. A secondary trench that exposed unfaulted deposits was located in the open field north of the station, and consisted of an excavation 23 meters long and 3 meters deep. The two trenches were separated by approximately 9 meters.

The ground surface at the west trench site was slightly lower than at the east trench. This slope to the west is consistent with a subtle south-west facing fault scarp. The thickness of surface fill increases from east to west, with pipe backfill associated with a City of Santa Rosa water pipeline encountered in the east end of Trench SCWA-T1 that partially obscures pre-existing geologic relations in the trench exposure.

4.3.1 Trench SCWA-T1 Stratigraphy

Trench SCWA-T2 exposes alluvial terrace and overbank deposits from nearby Santa Rosa Creek. Seven stratigraphic units (Units 100 through 610) were exposed in Trench SCWA-T1 (Figure 7, Table 3). Only three of the geologic units (Units 100, 200, and 300) are present in the eastern Trench SCWA-T2 with units 500 and 610 not present west of the fault at the depth of trenching and unit 600 below the depth of Trench SCWA-T2. The lower five units represent native materials exposed within the trench with the overlying material consisting of emplaced fill composed of clay with sand and pebbles. The fill thickens to the west from a few inches to up to a foot and a half and is assumed to have been placed during original development of the site. Pipeline trench backfill is present at the eastern end of the trench.

From youngest to oldest deposits, Unit 100 consists of dark grayish brown clay to silt, interpreted to be a slackwater deposit of Santa Rosa Creek. The unit fines upward with clay percentage decreasing with depth. This gradation, along with soil profile development, subdivides the unit into three distinct horizons. The AB soil horizon, uppermost, is the most clay-rich and has a weak blocky structure. The clay in this horizon is considered primary rather than pedogenic. The underlying ABt horizon has a weak to moderate angular blocky structure and common distinct clay films. The Bt horizon, lowermost, has moderate angular blocky structure and many distinct clay films. The clay films in the two lower horizons are likely pedogenic, derived from the upper horizon.

Beneath Unit 100 is a sequence of brown clay and gravelly fluvial deposits (Unit 200) likely deposited

by nearby Santa Rosa Creek. Fine to medium gravel, comprising 25% of the unit, is suspended in a matrix of sand, silt, and clay. This bed may be a debris flow or hyperconcentrated mudflow deposit. At the base of this deposit, many of the rounded to subangular gravel clasts are highly weathered. The gravels are predominately volcanic. No faulting or deformation was observed of the deposit or stratigraphic contacts bounding this or the overlying stratigraphic units within the western trench.

Unit 300 consists of bedded, highly weathered fluvial gravels with few distinct clay films, and are highly weathered. This deposit contains cobble-sized clasts that likely are fluvial terrace deposits of Santa Rosa Creek. Unit 400 consists of clayey gravel with rounded to sub-rounded cobbles predominately consisting of Sonoma Volcanics. This unit clearly is faulted and down-dropped to the west by the fault exposed between Stations 5 and 7.

Unit 500 consists of clayey gravel and cobbles composed of Sonoma Volcanics that is faulted between Stations 5 and 6 in Trench 1. Apparently down-dropped to the west, this unit is not exposed in the western portion of the trench.

Units 600 and 610 consist of dense silt to clay with minor gravel (basalt of the Sonoma Volcanics). Both units are faulted with unit 610 not exposed west of Station 6 in the trench. The apparent presence of Unit 600 west of Station 7 despite the absence of the overlying unit 500 gravels suggests that the fault offset cannot be primarily vertical (e.g. down to the west) and likely includes a significant strike-slip (lateral) component.

4.3.2 Trench SCWA-T1 Structural Features

The trench exposure exhibits fault features including truncated and downdropped beds, clay-filled vertical fractures that extended across the floor of the trench, and broad warping of fluvial units (Figure 9). Fault strands are mapped primarily on the basis of the truncation or displacement of bedding and the presence of vertical fractures.

The fault zone consisted of a vertical shear zone that was about 2.0 meters wide displaying apparent down-to-the-west displacement and an unknown amount of lateral displacement. A series of truncated and stratigraphically offset layers were documented within the fault zone. The base of both Unit 400 and Unit 300 can be correlated across the fault zone and are apparently downdropped vertically, approximately 1 m. Faulting may not have extended into Unit 300, which may be draped across a pre-existing fault scarp.

Table 1. Unit Descriptions, Trench FI-T-1

Unit No.	Description	Deposit
100	Lean CLAY with Sand and Gravel (CL); Dark Yellowish Brown 10YR (4/4); 20-25% fine to coarse, rounded to subangular sand; 20-25% rounded to subrounded gravel; 50-60% medium plasticity, medium toughness, no dilatancy fines; stratified to massive; volcanic sands and gravels; A horizon; clay film on clasts; fine roots throughout; gradual lower boundary	Fill
150	Clayey SILT; 2.5Y (3/1); 5% fine to medium, subangular to angular volcanic gravels; 15-20% fine to coarse subangular to angular sand; 75-80% hard, medium plasticity, low toughness, slow dilatancy, high dry strength fines; no soil structure; common fine pores (1 mm); common fine vertical white roots; clear, wavy lower boundary; A to AB horizon	Colluvium
160	Clayey SILT; 15-20% fine to medium, angular to subangular basalt and tuffaceous gravels; 25% fine to coarse, subangular to subrounded sand; 55-60% medium plasticity, medium toughness, slow dilatancy, high dry strength fines; common fine pores; rare roots; clear, wavy lower boundary; Bt soil horizon	Colluvium
180a	Silty CLAY; 2.5Y (3/1); <5% fine to medium, subangular to subrounded gravel; 5-10% fine to medium sand; 85-90% medium plasticity, medium toughness, slow dilatancy, high dry strength fines; massive; non-weathered; weak columnar to blocky peds; rare fine pores; rare fine roots; no clay film on clasts; gradual, smooth to wavy lower boundary	Colluvium
180	Clayey GRAVEL (GC); Dark Brown 10YR (2/2) to very dark grayish brown 10YR (3/2); 30-40% coarse, rounded to subangular gravel up to 50 cm; 45-55% medium plasticity, medium toughness, no dilatancy fines; 5-10% fine to medium sand; grades to finer grained colluvium (unit 170); matrix supported; massive; Bt horizon; clay film on clasts; vertically oriented gravels near fault plane; fine roots throughout; clasts are heavily weathered; wavy, gradational lower contact	Colluvium
200	Sandy Lean CLAY with Gravel (CL); Dark Yellowish Brown 10YR (3/4); 15% subrounded to subangular gravels; 20-30% fine to coarse, moderately graded, rounded to subangular sand; 55-65% medium plasticity, medium toughness, no dilatancy fines; volcanic sands and gravels up to 13 cm; stratified to massive; A-B horizon; granular; minor clay film on clasts; clear lower boundary; fine roots throughout; gravels are confined to lower 8 to 10 cm of unit	Colluvium
240	Clayey SILT with Sand and Gravel; 2.5Y (4/2); 5% subrounded to rounded cobbles; 10-15% fine to coarse, subangular to angular gravels; 5-10% medium to coarse subangular sand; 70-80% high plasticity, medium toughness, slow dilatancy, medium dry strength fines; massive; no soil structure; rare fine roots; gradual, wavy lower boundary	Colluvium
250	Lean CLAY with Sand and Gravel (CL); Olive Brown 2.5Y (4/3); soft; wet; 10-15% fine to medium sand; 10-15% coarse, rounded to subrounded gravel up to 17 cm; 70-80% medium plasticity, medium toughness, no dilatancy fines; massive; rare to no roots; Bt horizon; moderately to heavily weathered volcanic sand and gravel	Colluvium
300	Clayey SAND with Gravel (SC); Dark Brown 7.5YR (3/3); 20% subrounded to subangular gravel up to 6 to 8 cm; 30% medium plasticity, medium toughness, no dilatancy fines; 50% well-graded, fine to coarse, subrounded to angular sand; volcanic sands and gravels; stratified; Bt horizon; blocky to granular; fine roots in places; clay film on clasts; clasts are heavily weathered; lenses of fine sand are defining feature of unit, typically 6 to 8 cm thick	Alluvium
400	Lean CLAY with Sand and trace Gravel (CL); 5% medium, subangular to subrounded gravel; 10-15% fine to coarse, poorly graded, angular to subangular sand; 80-85%	Colluvium

	medium plasticity, medium toughness, no dilatancy fines; blocky; massive; volcanic lithics; sharp erosional lower contact; fine roots throughout.	
405	Lean CLAY (CL); Olive Brown 2.5Y (4/3); 98-100% medium toughness, medium plasticity, no dilatancy fines; <2% trace fine sand; stratified; Bt horizon; blocky; fine roots throughout; waxy texture on pedogenic faces; wavy, clear lower boundary	Alluvium
410	Lean CLAY with SILT (CL); Olive 5Y (5/3); soft, gouge material; wet; 95-100% medium toughness, medium plasticity, slow to no dilatancy fines; up to 5% fine sand; massive; Bt horizon?; gradational lower contact	Fault gouge
425	SILT with fine Sand (ML) interfingered with Clayey SAND (SC); Olive Brown 2.5Y (4/3) to Dark Yellowish Brown 10YR (4/4); upper and lower silt with fine sand packages consist of: 40-50% fine sand; 50-60% fines; stratified to massive; granular; wavy to irregular lower contact along lower silt package with heavy iron oxide staining; wavy lower contact with little to no iron oxide staining along upper silt package; interfingered clayey sand consist of: 5-15% rounded to subrounded gravel; 15% medium plasticity, medium toughness, no dilatancy fines; 70-80% poorly graded, fine to coarse, rounded to subangular sand; volcanic clasts; wavy lower contact; iron oxide staining along lower 17 to 25 cm of unit; stratified to massive.	Alluvium
450	Clayey SAND with Gravel (SC); Dark Yellowish Brown 10YR (4/4); 20% subrounded to subangular gravel; 30% medium plasticity, medium toughness, no dilatancy fines; 50% fine to coarse, rounded to angular sand; volcanic and sedimentary clasts; stratified; Bt horizon; blocky to granular; clay film on clasts; clasts are heavily weathered; thin lenses of sand present in unit 300 are absent; clear, wavy lower contact; Fluvial deposit	Alluvium
500	Lean CLAY (CL); Olive Brown 2.5Y (4/3); 98-100% medium toughness, medium plasticity, no dilatancy fines; 0-2% trace fine to medium sand; stratified; Bt horizon; blocky; fractures with silica? mineralization along fracture planes; waxy texture along pedogenic faces; wavy, clear lower boundary up to 2.5 cm; fine roots throughout	Alluvium
600	Lean CLAY with Sand with interbeds to lenses of Poorly Graded SAND with clay (CL to SP); Olive Brown 2.5Y (4/3); 40-50% medium toughness, medium plasticity, no dilatancy fines; 50-60% fine to coarse, subrounded to subangular sand; granite, quartz, basalt, chert and other volcanic lithics up to 1 cm diameter; trace gravels up to 5-7 cm; lenses of sand and gravel are up to 8 inches thick with iron oxide and manganese staining in places; stratified; Bt horizon; blocky; clay film and waxy surfaces on lithics; clasts are heavily weathered.	Alluvium

Table 2. Unit Descriptions, Trench FI-T-2

Unit No.	Description	Deposit
10	Lean CLAY with Sand and trace Gravel (ML); 5% coarse, subrounded volcanic gravels; 30% fine to medium sand; 65% medium toughness, medium plasticity fines; massive; A horizon; minor clay on clasts.	Fill, or reworked colluvium
20	Sandy Lean CLAY with SILT (CL); Dark Brown 7.5YR (3/3); 30-40% fine to coarse, poorly graded, subrounded to subangular volcanic clasts; 60-70% medium plasticity, medium toughness fines; A-B horizon; massive to blocky; fine roots throughout.	Colluvium
30	Sandy Lean CLAY with Gravel (CL); Dark Brown 7.5YR (3/3); 10-20% medium, subangular to subrounded gravel up to 15-cm; 30-40% medium plasticity, medium toughness fines; 40-50% fine to coarse, poorly graded, subrounded to subangular sand; massive; Bt horizon; volcanic lithics; heavily weathered clasts; fine roots throughout.	Colluvium
40	Sandy SILT with Gravel (ML); Brown 7.5YR (4/3); 20% coarse, subangular to subrounded gravel; 30% low plasticity, low toughness fines; 50% fine to coarse, poorly graded sand; massive; volcanic lithics; gravel up to 15-cm; fine roots throughout; root casts in places.	Colluvium
50	SILT with Sand and Clay (ML); Dark Brown 7.5YR (3/3); 30-40% fine sand; 60-70% low plasticity, low toughness, slow dilatancy fines; massive; Bt horizon; rare coarse, subangular volcanic gravel up to 5-cm; minor clay film on gravels.	Colluvium

Table 3. Unit Descriptions, Trench SCWA-T1

Unit No.	Description	Deposit
100	SILT with clay (ML), dark reddish brown 5YR (2.5/2) to very dark brown 10YR (2/2); massive; 0 to 2% coarse gravel; sub-rounded, volcanic; 98 to 100%, damp, low plasticity, soft, no dilatancy fines.	Alluvium
200	Base of brown clay in T-1 and T-2; CLAY (CL) with fine sand; dark reddish brown 5YR (2.5/2) to very dark brown 10YR (2/2); massive; 0 to 5% coarse gravel, sub-rounded to sub-angular, primarily Sonoma Volcanics; 5 to 10% fine, sub-rounded to sub-angular sand; 80 to 90% low to medium plasticity; damp (moisture decreases with depth), stiff, no dilatancy fines; soil ped structures apparent where moisture content is lower.	Alluvium
300	Clayey SAND (SC) with some coarse gravel; brown 7.5YR (4/4) to dark yellowish brown 10YR (3/6); 0 to 10% sub-rounded to sub-angular coarse gravel, generally weathered, primarily andesites and basalt (Sonoma volcanics); 10-20%, low plasticity, dry, hard, no dilatancy fines; 70 to 80% fine to medium, sub-angular to sub-rounded sand, indurated where dry, can form ped-like structures.	Alluvium
400	Clayey GRAVEL (GC); dark brown 7.5YR to 10YR (3/3); 20% rounded to sub-rounded gravel, clasts up to 23 cm, basalts and andesites (Sonoma Volcanics), clay films on some clasts; clasts heavily weathered; 30 to 40% medium plasticity, moist, soft, no dilatancy fines; 50% fine to coarse, sub-angular to rounded sand, fines upwards.	Alluvium
500	Clayey GRAVEL (GC); dark brown 7.5YR to 10YR (3/3); 20 to 30% medium plasticity, moist, soft, no dilatancy fines; 30% rounded to sub-rounded gravel, cobbles up to approximately 30 cm, basalts and andesites (Sonoma Volcanics), clay films on some clasts; clasts heavily weathered; 40% fine to coarse, sub-angular to rounded sand.	Alluvium
600	SILT (ML) with some sand; pale yellow 2.5YR (7/4) to light yellowish brown 2.5YR (6/4); <5% coarse, sub-rounded to sub-angular sand, up to 4 mm; 95% low plasticity, damp, soft, no dilatancy fines; thin brownish clay coating visible where roots are present.	Alluvium
610	CLAY with silt (CL); reddish brown 5YR (4/4) to brown 7.5YR (4/4); <1% sub-rounded to sub-angular gravel, up to 2 cm, basalt (Sonoma Volcanics); 99 to 100% low to medium plasticity, moist, soft, no dilatancy fines.	Alluvium

5.0 DEPOSIT AGE ESTIMATES

Ages of the surficial deposits at the Spring Valley trenches are estimated through assessment of soil profile development in trenches FI-T-1 and SCWA-T-1, and radiocarbon analysis of six bulk soil samples from trench FI-T-1. Methods, results, and interpretations are presented below.

5.1 Geochronologic Methods

Soil profile descriptions were completed at two locations in trench FI-T-1 and within trench SCWA-T1. Soil-profile locations were selected collaboratively by the team. Soil profiles were described using standard soil description methods (Birkeland 1999; Schoenberger et al. 2002) and data were entered on a data capture form. A sketch was made and a photograph taken of each profile. An interpretation of the soil profile development was then made, emphasizing features of the soil that helped tell the story of landscape evolution, past environments, and faulting history at each respective site.

A total of six bulk soil samples from trench FI-T-1 were submitted to PaleoResearch Institute for radiocarbon analysis using accelerator mass spectrometry (AMS). The bulk samples, collected from colluvial units on either side of the fault zone (Figure 9), were submitted for macrofloral analysis to recover charred remains suitable for AMS radiocarbon analysis. No samples of the fluvial deposits were collected as they were judged unlikely to contain datable material and likely to be older than the maximum limit of the radiocarbon method. Based on low yield of charcoal by standard separation techniques, microscopic charcoal recovery was performed for three of these sediments. Three charred remains and three microcharcoal samples were submitted for AMS radiocarbon age determination (Table 4).

Table 4. Radiocarbon Sample Collection

Sample Number	No. of Bags	Station (m)*	Depth (m)	Unit	Date collected	By
1	1	Station 26.5	0.58	200	10/29/2015	Kelsey/ Mayo
2	3	Station 29.1	0.79	150	11/5/2015	Kelsey/Mayo
3	1	Station 27.5	0.82	180	10/29/2015	Kelsey/Mayo
4	1	Station 25	0.81	400	11/5/2015	Hoeft/Hitchcock
5	1	Station 27.5	1.14	180	11/5/2015	Hoeft/Hitchcock
6	1	Station 30.2	1.19	160	11/5/2015	Hoeft/Hitchcock
*Sample locations are shown on the log of trench FI-T-1 (Figure 9 and Plate 1)						

5.2 Geochronology Results

Soil geochronology and radiocarbon analysis show that geologic units range in age from late Pleistocene through late Holocene. Fluvial deposits observed in trench FI-T-1 and SCWA-T-1 are the oldest materials, their Late Pleistocene ages estimated from soil profile development. Radiocarbon ages of colluvial deposits in trench FI-T-1 fall within the Holocene, consistent with Holocene age estimates from soil profile development within the colluvial units. Results are described in detail below.

5.2.1 Soil Profile Development

Soil profile development was assessed through the description and interpretation of three soil profiles: two profiles in trench FI-T-1, and one profile in trench SCWA-T-1. Soils were described in the field using the methods of the U. S. Department of Agriculture (Schoenberger and others, 2012).

Soil profile 1 is located at station 8.5 in trench FI-T-1, within the fluvial terrace deposit sequence (Plate 1). The 260-cm-deep profile consists of a layer of fill, over a moderately developed soil profile in gravelly colluvium and alluvium, over a deeply weathered mature buried soil profile developed in sandy and gravelly alluvium. Features of the upper soil profile (55 to 114 cm depth) include an A horizon of gravelly fine sandy loam, underlain by a weak Bt horizon of silty fine gravel and coarse sand with few faint clay films on ped faces, patches of manganese, and weathered clasts.

The mature buried soil in soil profile 1 (114 to 260 cm) features a truncated AB horizon of dark gray clay with strong prismatic structure and abundant distinct clay films, underlain by a Btq horizon of sandy clay loam. This Btq horizon is distinct for its abundant prominent clay films and prominent fractures lined with a very pale brown mineral coating ($\leq$ 1 mm thick), assumed to be silica formed by weathering of volcanic detritus in the alluvium. The fractures are dominantly subvertical and may extend partially into the underlying Bt horizons. Below the Btq horizon are the Bt1 and Bt2 horizons which feature prominent clay films gradually decreasing in abundance with depth. Both lack the abundant mineralized fractures. The Bt2 horizon is developed within a fine gravelly bed in the alluvium, illustrated on the geologic log (Plate 1). Beneath the Bt2 horizon is the 2C horizon of clayey sandy silt to silty sand in which clay films are few and clay appears to be dominantly primary in origin.

The mature soil profile developed below 114 cm in soil profile 1 is consistent with a late Pleistocene age (~10,000 to 100,000 years). The overlying moderately developed soil profile from 55 to 114 cm is consistent with an early to middle Holocene age (10,000 to 4,000 years).

Soil profile 2 is located at station 29.5 in trench FI-T-1, within a thick sequence of colluvial deposits on the west side of the fault. The 276-cm-deep profile consists of 60 cm of fill over two weakly to moderately developed soil profiles. The upper soil, 60 to 174 cm depth, consists of a silt loam A horizon, a transitional AB horizon of gravelly clay loam, and an underlying Bt horizon of gravelly clay loam with weak prismatic structure and few faint clay films. The soil profile development in the upper soil is consistent with a late Holocene age.

A moderately developed soil (174 to 276 cm) underlies the upper soil in soil profile 2. This soil features a 2ABt horizon of silty clay loam with strong blocky structure and abundant prominent clay films, with root tracks on the ped faces. The 2ABt horizon is underlain by the 2Bt1 horizon of clay loam with gravel, abundant distinct clay films, and moderate blocky structure. Below this, the 2Bt2 horizon is a fine sandy silt with gravel, massive, with common distinct clay films. The soil profile development in the lower soil is consistent with an early to middle Holocene age.

Soil profile SCWA-SP-2 is located at station 16 m on the south wall of trench SCWA-T-1. The trench was about 32 inches wide and 2.65 m deep at this location. This soil profile consists of three distinct units.

Beneath a 10.5 cm layer of gravelly fill, the upper unit consists of a 60 cm-thick layer of very dark brown fine sandy silt, interpreted as overbank deposits of Santa Rosa Creek. This unit is massive and very friable, and exhibits little soil profile development. The unit is subdivided into two horizons, A1 and A2, based on the slightly darker color of the upper horizon (A1), reflecting relatively greater accumulation of organic matter. The A1 horizon also has common fine roots. The base of the A2 horizon abruptly contacts the unit below.

From 70 cm to 131 cm depth, is a 61-cm thick unit of very dark grayish brown clay. This clay is interpreted to be a slackwater deposit of Santa Rosa Creek. The unit is subdivided into two horizons, 2Bt1 and 2Bt2, on the basis of the presence of strong prismatic structure and faint clay films in the lower horizon.

Beneath the clay, from a depth of 131 cm to the bottom of the trench at 272 cm, is a sequence of gravelly and sandy fluvial deposits of Santa Rosa Creek. Similar to SP-2, the uppermost unit is poorly sorted, massive, weathered gravelly sandy clay loam, interpreted as a debris flow deposit. Gravel clasts are weathered, and the matrix has scattered iron and manganese coatings and segregations. The next bed is a gravelly sand, stratified, with coarser clasts than above and very little clay. Gravel clasts are weathered. Finally, at the base of the fluvial sequence is a bed of sand which interfingers with the gravel. The sand is massive in structure, and also weathered.

This soil profile in the SCWA trench reflects a history of deposition by Santa Rosa Creek and weathering and soil profile development of the deposits. The uppermost unit, consisting of fine sand silt overbank deposits, is the youngest unit and based on its stratigraphic positions and lack of soil profile development except for organic matter accumulation, is estimated to be late Holocene in age (4,000 to present). The clay unit, seen in both soil profiles, exhibits soil profile development consistent with an early to middle Holocene age of 12,000 to 4,000 years. The fluvial gravels and sands, based on the highly weathered nature of many of the gravel clasts, and the presence of manganese and iron coatings, may be latest Pleistocene in age, approximately 12,000 to 30,000 years. Due to the many factors that can affect the rates of soil profile development, age estimates should be considered approximate.

5.2.2 AMS Radiocarbon Results

Radiocarbon ages for the six samples from trench FI-T-1 indicate that all colluvial deposits sampled are of Holocene age (Table 5), a result consistent with estimates based on soil profile development. Specific ages for the six samples, however, show stratigraphic inconsistencies which warrant examination and selection, based on geologic judgement, of the most reliable age results.

The relative ages of the six samples based on stratigraphic position (Figure 9), should be in the following order (oldest to youngest): sample 4, sample 1, samples 3 and 5, sample 6, sample 2 (Figure 9). Sample 4 does indeed yield the oldest radiocarbon age, therefore its age of 7,160-6,890 cal yr BP, is accepted as the best age estimate for unit 400, its host unit.

The ages for samples 1, 3, and 5 should be similar to one another, as their host units, 200 and 180, are considered to be downfaulted equivalents. Their ages are quite dissimilar, however. The young age of sample 1 (520-320 cal yr BP) likely reflects incorporation of modern surficial organic matter, based on its shallow depth, thus its result is discarded. Samples 3 and 5 ages were taken from the same unit

within 30 cm of one another, yet their radiocarbon results are also dissimilar. Sample 3 is chosen as the less reliable of the two, as the quantity of charcoal obtained from the bulk sample was very small, and the age result is younger than the results from both stratigraphically overlying units. Thus, the best age estimate for unit 180 is judged to be the radiocarbon result for sample 5 of 3,000-2,860 cal. yr BP.

The radiocarbon ages of samples 2 and 6 are inconsistent with the stratigraphic position of their host deposits, units 160 and 150. The age result for sample 6 is also inconsistent with the "best estimate" age of underlying unit 180. Thus, the age result for sample 6 is discarded, and presumed to reflect some reincorporation of older detrital charcoal. The age result for sample 2, at 2,310-2,120 cal yr BP**,** is therefore judged to be the best age estimate for unit 150. This sample was of high quality and consisted of charred Quercus remains.

In summary, the radiocarbon results yielded three age estimates judged to be reliable, in correct stratigraphic order, and likely to reflect the age of deposition. These age estimates, for samples 2, 4, and 5, are shown in **boldface** type in Table 5, and for the framework for a chronology of faulting events in trench FI-T-1, presented in Section 6.

Table 5. AMS Radiocarbon Results

Field sample number	Lab sample number*	Host unit in trench stratigraphy	Lab reported age, ^{14}C year BP*	Calibrated age range (2 sigma) yr BP: Years before AD1950**	Material*
1	5534	Unit 200	399±27	520-320	Small, vitrified unidentified charcoal fragments
2	5363	Unit 150	2,178±23	**2,310-2,120** [1]	Oak (Quercus) charcoal
3	5535	Unit 180	1,662±29	1,690-1,420	Small, vitrified unidentified charcoal fragments
4	5537	Unit 400	6,115±25	**7,160-6,890** [1]	Microscopic charcoal extracted from retained flotation sediment
5	5364	Unit 180	2,830±24	**3,000-2,860** [1]	Microscopic charcoal extracted from retained flotation sediment
6	5536	Unit 160	4,192±24	4,840-4,620	Microscopic charcoal extracted from retained flotation sediment

Note:

*Samples were processed by PaleoResearch Institute, Golden CO and then sent to The Center for Applied Isotope Studies in Athens (CAIS), Georgia, where the CO_2 gas was processed into graphite. The graphitized samples were placed in the target and run through the accelerator, generating numbers that are subsequently converted into radiocarbon ages.

**Ages were calibrated (2 sigma) using IntCal13 curves on OxCal version 4.2.4 (Bronk Ramsey and Lee 2013; Bronk Ramsey 2009; Reimer et al. 2013).

[1]Results in **bold** are used to constrain the event chronology.

6.0 INTERPRETATION AND DISCUSSION

The results of this study represent significant progress in characterizing the presence, geometry, and history of faulting on the Spring Valley strand of the Bennett Valley fault. Of the four trenches excavated, two provide clear evidence of Quaternary fault displacement. Geochronologic data collected in trench FI-T-1 show that the most recent fault displacement took place in the Holocene.

6.1 Interpretation of Trench FI-T-1

The fault zone exposed in Trench FI-T-1 consists of a near-vertical shear zone displaying apparent down-to-the-west displacement. The dip of the fault plane in the trench wall is about 80 degrees west. Combined with the linear nature of the mapped fault, significant lateral displacement is inferred. Vertical displacement, measured from the base of unit 240 on the downthrown side to the base of unit 400 on the upthrown side, is 1 to 1.5 meters over the past approximately 7,000 years (sample 4, Table 5).

The chronology of past earthquakes has been reconstructed based on cross-cutting relationships and available geochronologic data (Table 5). The chronology is summarized in Table 6. The earliest earthquake (Faulting Event 1) for which this trench provides evidence occurred in the late Pleistocene and is inferred based on the observed folding of unit 425. The folding was followed by a period of erosion which truncated the fold. Fluvial unit 400 was deposited over the eroded fold during the Early Holocene, based on a radiocarbon age for unit 400 of 7,160-6,890 cal yr. BP.

In the next earthquake, Faulting Event 2, Unit 400 and underlying units are faulted, and scarp colluvial unit 240 is deposited. Portions of unit 240 adjacent to the fault may constitute downfaulted blocks of unit 400, further from the fault zone unit 240 is a colluvial deposit derived from unit 400. The relationship is not clear, which may reflect significant lateral displacement.

Unit 200 is offset by Faulting Event 3. This event resulted in deposition of colluvium unit 180, inferred to be derived from erosion of the scarp.

The penultimate earthquake (Faulting Event 4) offsets unit 180. Unit 180 has two 14C age determinations: 3,000-2,860 yr BP (sample 5) and 1,690-1,420 yr BP (Table 5; sample 3). However, sample 3 is out of order compared with the age from unit 150 (sample 2), is located stratigraphically higher within the root zone and, therefore, considered less reliable. Faulting Event 3 therefore likely occurred after 3,000-2,860 yr BP.

The most recent earthquake (Faulting Event 5) likely resulted in deposition of colluvium 150, deposited on top of folded colluvium 160. We do not know if colluviums 160 and 150 are offset by faults because the source strata for these colluvial deposits have been removed either by natural erosion or blading during landscaping that accompanied dam construction. Support for Faulting Event 5 includes:

1. Unit 160 appears folded (i.e., event 5) then truncated by unit 150;
2. The geometry of colluvial unit 180 is consistent with unit being folded then refolded, i.e., folding during two successive earthquakes with the first folding (i.e., event 4) simultaneous with the fault truncation of this unit and the second folding (i.e., event 5) simultaneous with the first folding of overlying unto 160.

There are two ages derived from colluvium units 150 and 160 with the youngest age, sample 2, unit 150 (2310-2120 cal yr BP) likely detrital, under the reasoning that one takes the youngest detrital age out of

a set of detrital ages from the same sample space. Because earthquake 5 occurred before deposition of colluvium 150, Fault Event 5 occurred before 2,310-2,120 yr BP.

In summary, we interpret a maximum of four and minimum of three Holocene earthquakes within the past seven thousand years, with the most recent earthquake occurring before 2,310-2,120 years ago. An older earthquake likely occurred in the late Pleistocene, and is inferred based on folding of unit 425.

If we assume four Holocene earthquakes, the average time between earthquakes in the Holocene is about 1,530-1,680 years. Reasoning: The sampled interval is about 4,580-5,040 years (time between earthquakes #2 and #5). In this interval, there were four earthquakes and three inter-earthquake periods. Hence, 4580/3 = 1530 years; 5040/3=1680).

Table 6. Chronology of Events, Trench FI-T-1

Time, oldest to youngest	Geologic Event
Late Pleistocene	Fluvial deposition of units 500 and 600 by Santa Rosa Creek
	Soil profile development
	Fluvial deposition of unit 425 by Santa Rosa Creek
	Folding of unit 425: **Faulting Event 1**
	Erosion, truncating units 425 and 500
Early Holocene	Deposition of alluvial unit 400
	Faulting of alluvial unit 400, **Faulting Event 2**
	Deposition of scarp colluvium 240
	Soil profile development
	Deposition of alluvial unit 200
	Faulting of alluvial unit 200, **Faulting Event 3**
Late Holocene	Deposition of scarp colluvium 180
	Fault offset of unit 180: **Faulting Event 4**
	Deposition of colluvium 160 and 150
	Apparent folding of unit 160: **Possible faulting Event 5**
	Soil profile development
Historical	Grading and fill emplacement

6.2 Interpretation of Trench FI-T-2

Three possible interpretations are considered for the lack of faulting evidence in trench FI-T-2. First, the trench may miss the fault, and the fault is located to the east or the west of the trench excavation. Second, the fault is indeed present at depth and a surface rupturing event has not taken place that post-dates the deposition of the colluvial units exposed in the trench. In this case, fault activity may not be uniform between the north and south sites, or the deposits at the southern site may be younger than those at the northern site.

Third, minor displacement has been obliterated by shrinking and swelling of the clay-rich soils. Consistent with this third possibility, the top of unit 40 exhibits a convexity at station 5 and concavity at station 10 that could be interpreted as a monoclinal fold or a modified fault scarp. Further work at other locations along the fault is needed to evaluate these three possibilities.

6.3 Interpretation of Trench SCWA-T1

The fault is clearly expressed and Faulting is observed to displace the late Pleistocene deposits and may also deform the Holocene deposits. Consistent with observations in trench FI-T-1, apparent displacement due to faulting is down-to-the-west. Lateral movement is suspected but could not be documented from the available exposures.

The mature soil profile developed below 114 cm in the soil profile within faulted units exposed trench SCWA-T1 is consistent with a late Pleistocene age (~10,000 to 100,000 years). The overlying moderately developed soil profile from 55 to 114 cm is consistent with an early to middle Holocene age (10,000 to 4,000 years).

7.0 CONCLUSIONS

This study establishes the presence of Holocene faulting along the Spring Valley strand of the Bennett Valley fault. The fault is clearly expressed in two trench exposures, FI-T-1 and SCWA-T1, and is observed to dip steeply to the west. Late Pleistocene fluvial units and Holocene colluvial units are truncated or displaced against the fault. Fluvial units are monoclinally folded on the hanging wall of the fault.

In trench FI-T-1, colluvial units yield middle to late Holocene radiocarbon ages, suggesting the fault may be active. The presence of microseismicity along the Spring Valley strand supports this possibility. We infer four to five faulting events based on the stratigraphy, fault truncations, and cross cutting relationships. Three to four of these events affect Holocene deposits.

Additional information on the Holocene history of rupture events at additional sites along the Spring Valley fault is needed to refine the timing of the most recent event and more broadly to help better understand the behavior of this potentially important fault. In addition, a better understanding of the along-strike characteristics of the active trace and the nature of its connection at either end to master faults such as the Bennett Valley, Maacama, or Rodgers Creek faults, is key to identifying potential rupture scenarios that may impact the Santa Rosa metropolitan area.

This information for the Spring Valley strand may lead to improvements in the source characterization for future iterations of probabilistic ground motion maps. Specifically, understanding the amount of slip transferred along the Spring Valley strand from the Rodgers Creek fault to the Maacama fault directly

impacts the seismic hazard to downtown Santa Rosa, which is underlain by the Rodgers Creek fault (Figure 1). If significant strain is accommodated by the Spring Valley fault, the associated surface rupture hazard (i.e. amount of lateral offset) associated with the Rodgers Creek fault may be lower for the poorly defined Rodgers Creek fault mapped beneath the downtown Santa Rosa area.

ACKNOWLEDGEMENTS

Primary funding for the project was provided by the U.S. Geological Survey's National Earthquake Hazard Reduction Program under grant awards G15AP00064 and G15AP00065. The Sonoma County Water Agency (SCWA) funded the study of the northern strand of the Spring Valley fault. We thank Mike West, Ken Gylfe, and Jay Jasperse at the SCWA for permission to share data from this site-specific consulting study.

Sonoma County Parks gave permission for the excavation of the two trenches within Spring Lake Park. Park staff Fernando Espinosa provided guidance on requirements to ensure public safety of park visitors, and shared information regarding the seeps that appeared after the 2014 South Napa earthquake.

USGS colleagues Robert McLaughlin, Suzanne Hecker, Carol Prentice, and Jack Boatwright were key supporters of the scientific objectives of the project and we thank them for many helpful discussions, field visits, field reviews, and logistical support to complete the project successfully. We also thank Gordon Seitz of the California Geological Survey for comments during his field review of the SCWA trenches. Peter Berger coordinated additional logistical support within Fugro for this study. Zach Mayo, Adam Wade, Cooper Brossy, David Trench, and Danielle Madugo provided field support for this study.

REFERENCES

Budding, K. E., Schwartz, D., and Oppenheimer, D. H., 1991, Slip rate, earthquake recurrence, and seismogenic potential of the Rodgers Creek fault zone, northern California: Initial results: Geophysical Research Letters, v. 18, p. 447-450.

Hart, E.W., 1990, Fault-rupture hazard zones in California, California Division of Mines and Geology Publication 42, 26 p.

Hecker, Suzanne, 2010, Mapping of the Rodgers Creek fault from LiDAR data: unpublished GIS files obtained from the author.

Hecker, S., Kelsey, H. M., and sixteen others, 2006, History and pre-history of earthquakes in wine and redwood country, Sonoma and Mendocino counties, California, *in* Prentice, C., S., Scotchmoore, J. G., Moores, E. M., and Kiland, J. P., eds. San Francisco Earthquake Centennial Field Guides: Field trips associated with the 100th Anniversary Conference, 18-23 April, San Francisco, California; geological Society of America Field Guide 7, p. 339-372, doi: 10.1130/2006.1906SF(19).

Hitchcock, C.S., 2006, Preliminary mapping for the system-wide reliability study: Sonoma County Water Agency unpublished consultant report.

Langenheim, V. E., Graymer, R. W., Jachens, R. C., McLaughlin, R. J., Wagner, D. L., and Sweetkind, D. S., 2010, Geophysical framework of the northern San Francisco Bay region, California: Geosphere, v. 6, no 5., p. 594-620.

McLaughlin, R. J., Sarna-Wojcicki, A. M., Fleck, R. J., Wright, W. H., Levin, V. R. G, and Valin, Z. C., 2004a, Geology, tephrochronology, radiometric ages, and cross sections of the Mark West Springs 7.5' quadrangle, Sonoma and Napa Counties, California: U. S. Geological Survey Scientific Investigations Map 2858.

McLaughlin, R. J., Sarna-Wojcicki, A. M., Fleck, Jachens, R. C., Langenheim, V., McPhee, D. K., Wentworth, C. M., Roberts, C., McCabe, C. A., and Valin, Z. C., 2004b, Geology of the right step from the Rodgers Creek fault to the Maacama fault, northern San Francisco Bay region, California: Pliocene-Quaternary slip rates and preliminary 3D model: in USGS NEHRP Research Summaries, Northern California Earthquake Hazards, FY 2004.

McLaughlin, R.J., Langenheim, V.E., Sarna-Wojcicki, Fleck, R.J., McFee, D.K., Roberts, C.W., McCabe, C.A., and Wan, Elmira, 2008, Geologic and geophysical framework of the Santa Rosa 7.5' quadrangle, Sonoma County, California: U. S. Geological Survey Open-File Report 2008-1009.

McLaughlin, Robert J., Sarna-Wojcicki, Andrei M., Wagner, David L., Fleck, Robert J., Langenheim, Victoria E., Jachens, Robert C., Clahan, Kevin and Allen, James R., 2012, Evolution of the Rodgers Creek-Maacama right-lateral fault system and associated basins east of the northward-migrating Mendocino Triple Junction, northern California: Geosphere, v.8, p. 342-373; doi: 10.1130/ GES00682.1

Schoenberger, P. J., Wysocki, D. A., Benham, E. C., and Broderson, W. D. (editors), 2012, Field book for describing and sampling soils, Version 2.0, Natural Resources Conservation Service, National Soil Survey Center, Lincoln, NE.

Schwartz, D. P., Pantosti, D., Hecker, S., Okumura, K., Budding, K. E., and Powers, T., 1992, Late Holocene behavior and seismogenic potential of the Rodgers Creek fault zone, Sonoma County, California: *in*: Proceedings of the Second Conference on Earthquake Hazards in the Eastern San

Francisco Bay Area, Proceedings, California Division of Mines and Geology Special Publication 113, p 393-398.

Sowers, J. M., Hoeft, J. S., and Kelsey, H. M., 2009, Mapping, Assessment, and Digital Compilation of the Southern Maacama Fault, Sonoma County, for the Northern California Quaternary Fault Map Database: Collaborative Research with William Lettis & Associates, Inc., and the U.S. Geological Survey: Final Technical Report, U. S. Geological Survey NEHRP grant award #08HQGR0056, 25 pages, 9 plates, GIS database.

Sowers, J. M., Kelsey, H. M., and Unruh, J. R., 2010, Mapping, Assessment, and Digital Compilation of the Connection Between the Rodgers Creek and Maacama Faults, Sonoma County, for the Northern California Quaternary Fault Map Database: Collaborative Research with William Lettis & Associates, Inc., and the U.S. Geological Survey. Final Technical Report, U. S. Geological Survey NEHRP grant award #G09AP00058.

U. S. Department of Agriculture, 1942, Black and white aerial photography, 1:20,000-scale, series COF-7, COF-14, and COF-15.

U.S. Geological Survey and California Geological Survey, 2009, Quaternary fault and fold database for the United States, accessed March 2010, from USGS web site: http://earthquakes.usgs.gov/regional/qfaults/.

Wagner, D. L., and Bortugno, E., 1982, Geologic Map of the Santa Rosa Quadrangle, California, 1:250,000: California Division of Mines and Geology.

Waldhauser, F., and W.L. Ellsworth, 2000, A double-difference earthquake location algorithm; method and application to the northern Hayward Fault, California: Bulletin of the Seismological Society of America, v. 90, p. 1353-1368.

Waldhauser, F., and D. P. Schaff (2008), Large-scale relocation of two decades of Northern California seismicity using cross-correlation and double-difference methods, J. Geophys. Res., 113, B08311, doi:10.1029/2007JB005479. Double-difference Earthquake Catalog for Northern California (1984-2011) downloaded Nov 7, 2016 from: http://www.ldeo.columbia.edu/~felixw/NCAeqDD/, and updated through 2016 from http://ddrt.ldeo.columbia.edu/DDRT/index.html.

Wong, I.G., and Bott, J.D.J, 1995, A new look back at the 1969 Santa Rosa, California, earthquakes: Bulletin of the Seismological Society of America, v. 85, no. 1, p. 334-341.

Working Group on California Earthquake Probabilities (WGCEP), 2003, Earthquake Probabilities in the San Francisco Bay Region: 2002–2031: U. S. Geological Survey Open-File Report 03-214.

Bibliography of reports resulting from the work performed under this award:

Sowers, J. M., Hitchcock, C. H., Hoeft, J. S., Barron, A., Kelsey, H., Brossy, C., and Mayo, Z., 2016, Paleoseismic Investigation of the Spring Valley fault, Santa Rosa, California: Evidence for Holocene Activity (Abstract): American Geophysical Union Fall Meeting, San Francisco, CA**.**

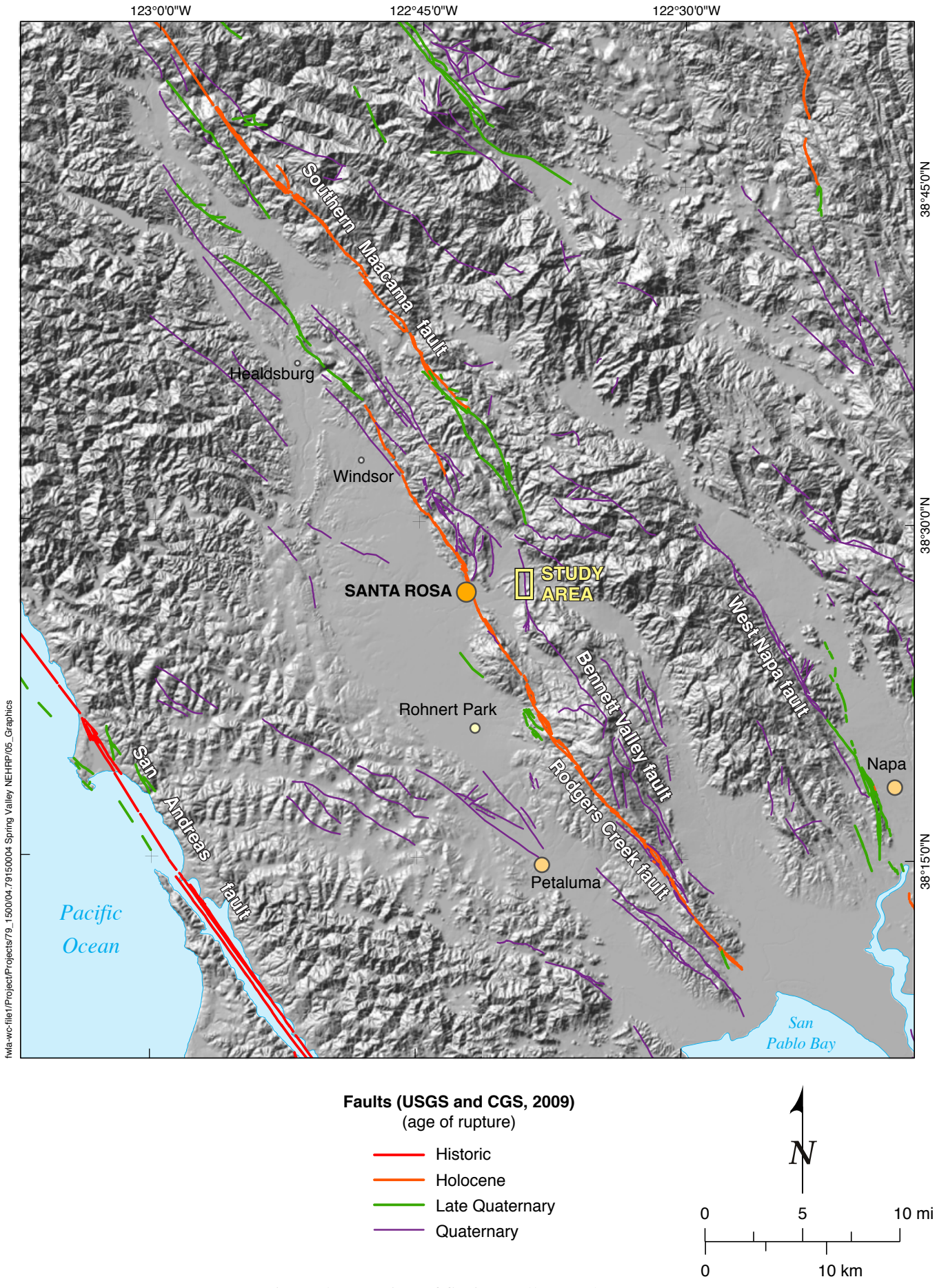

Figure 1. Location of Spring Valley study area.

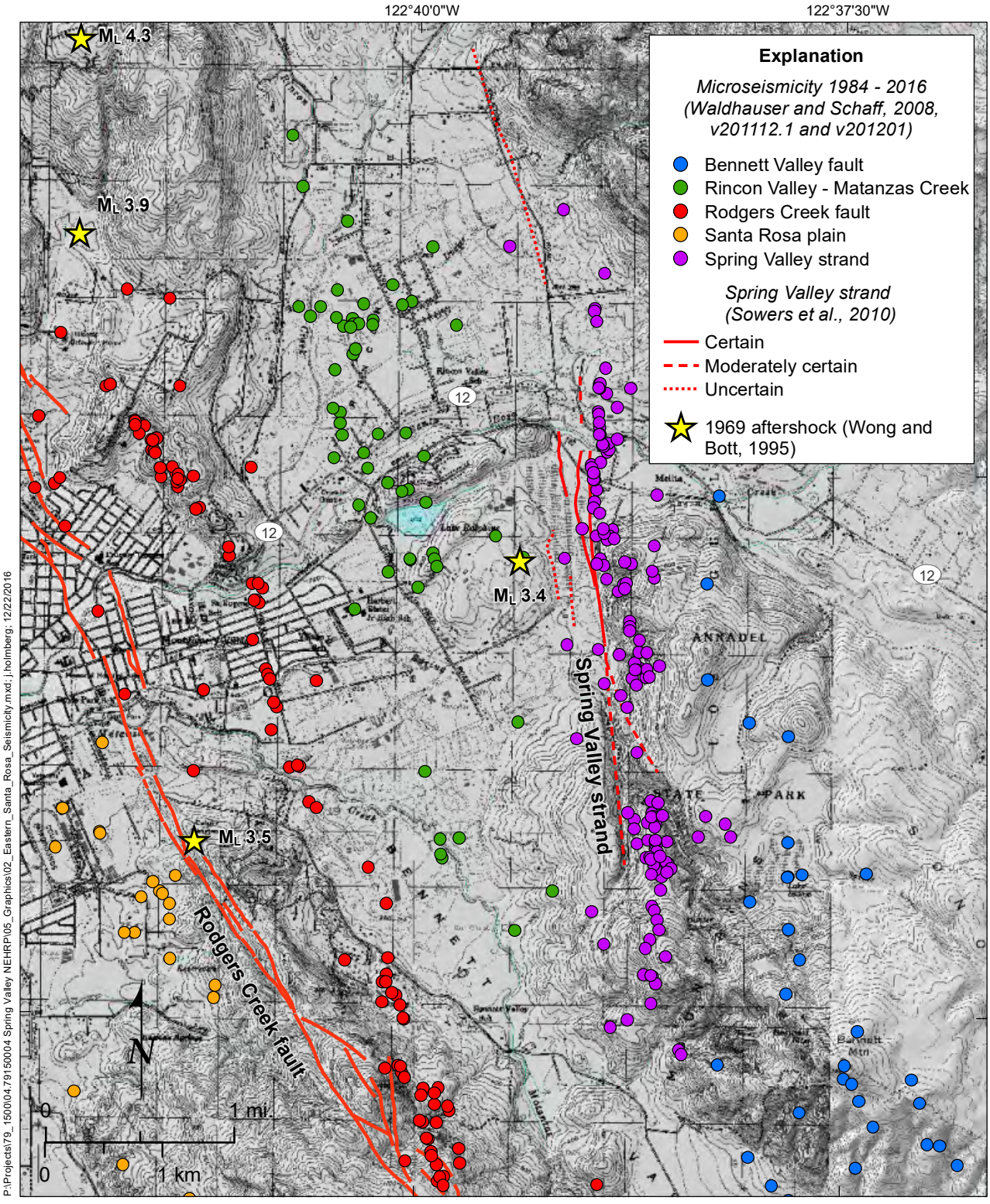

Figure 2. Eastern Santa Rosa seismicity.

Sources: 1. USDA 1942 COF-14-25 aerial photograph.
2. USGS 10-meter DEM hillshade.

Figure 3. 1942 aerial photograph of Spring Valley area.

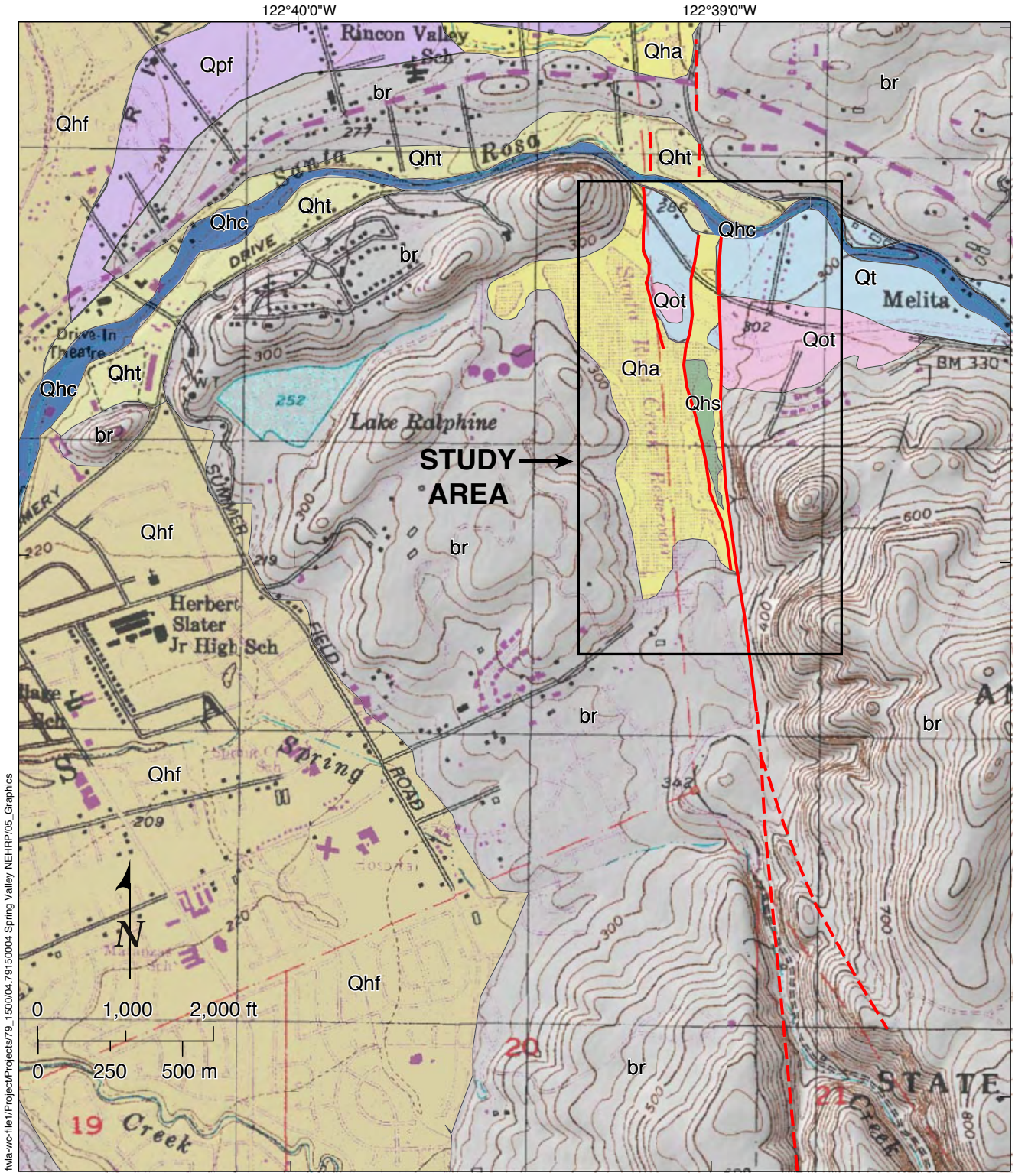

Sources: 1. Geology and Faults: Sowers et al., 2010.
2. Base map: USGS 7.5-minute topographic map.

Explanation

- Fault; dashed where less certain
- Qhc — Historical stream channel deposits
- Qht — Holocene terrace deposits
- Qha — Holocene alluvium
- Qhs — Historical marsh deposits
- Qhf — Holocene alluvial fan deposits
- Qt — Late Pleistocene to Holocene terrace deposits
- Qpf — Pleistocene alluvial fan deposits
- Qot — Pleistocene terrace deposits
- br — Bedrock and colluvium

Figure 4. Fault features and Quaternary geology of Spring Valley area.

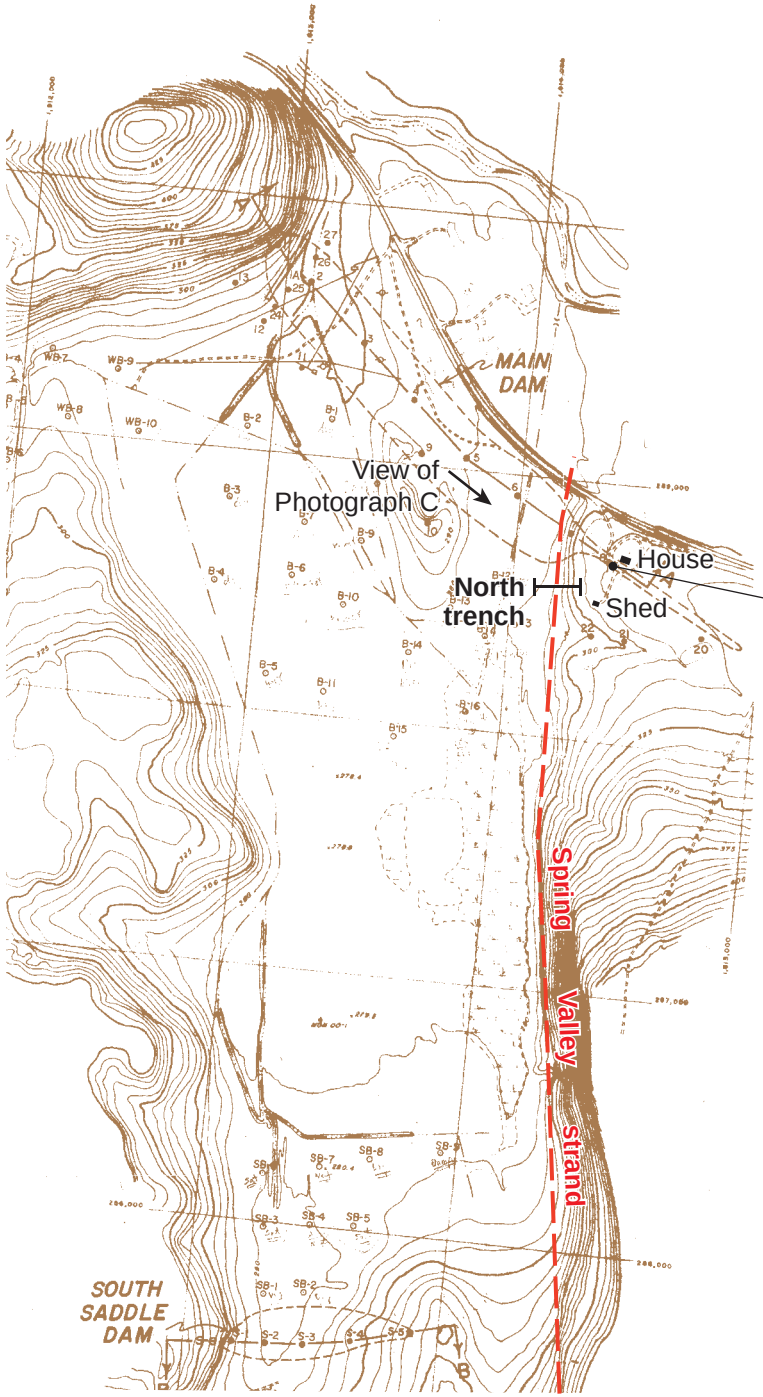

A)

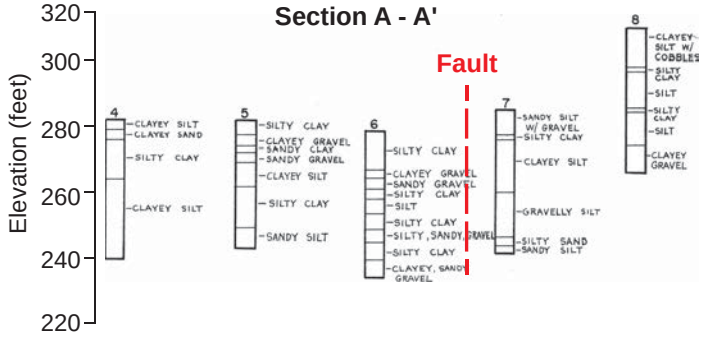

East-west borehole transect across fault

B)

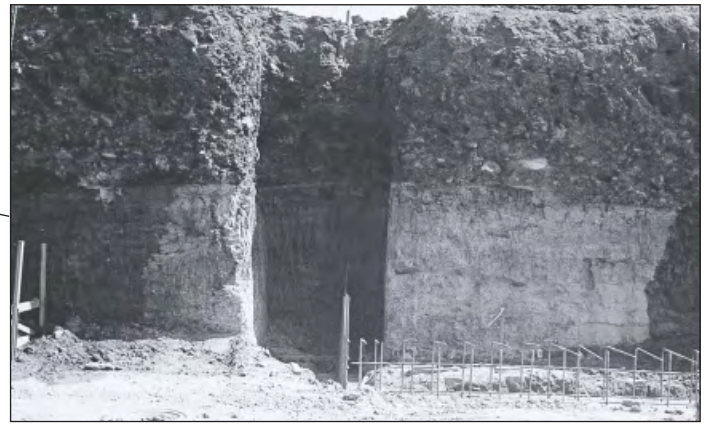

Photograph of stream terrace exposure in emergency spillway excavation

C)

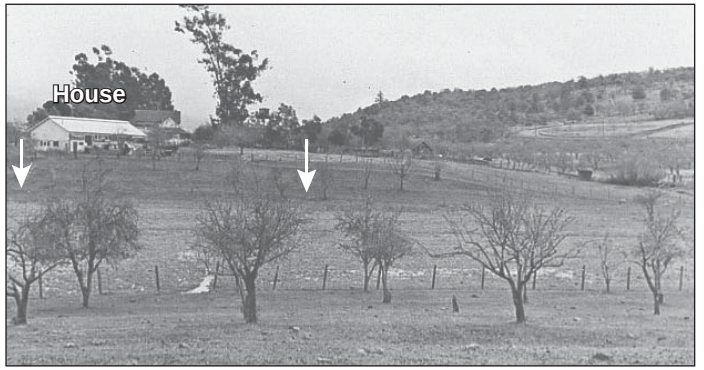

Pre-construction photograph looking southeast showing scarp (arrows), near proposed north trench site

Figure 5. Proposed north trench area showing topography, boring transect, and photographs, circa 1962.

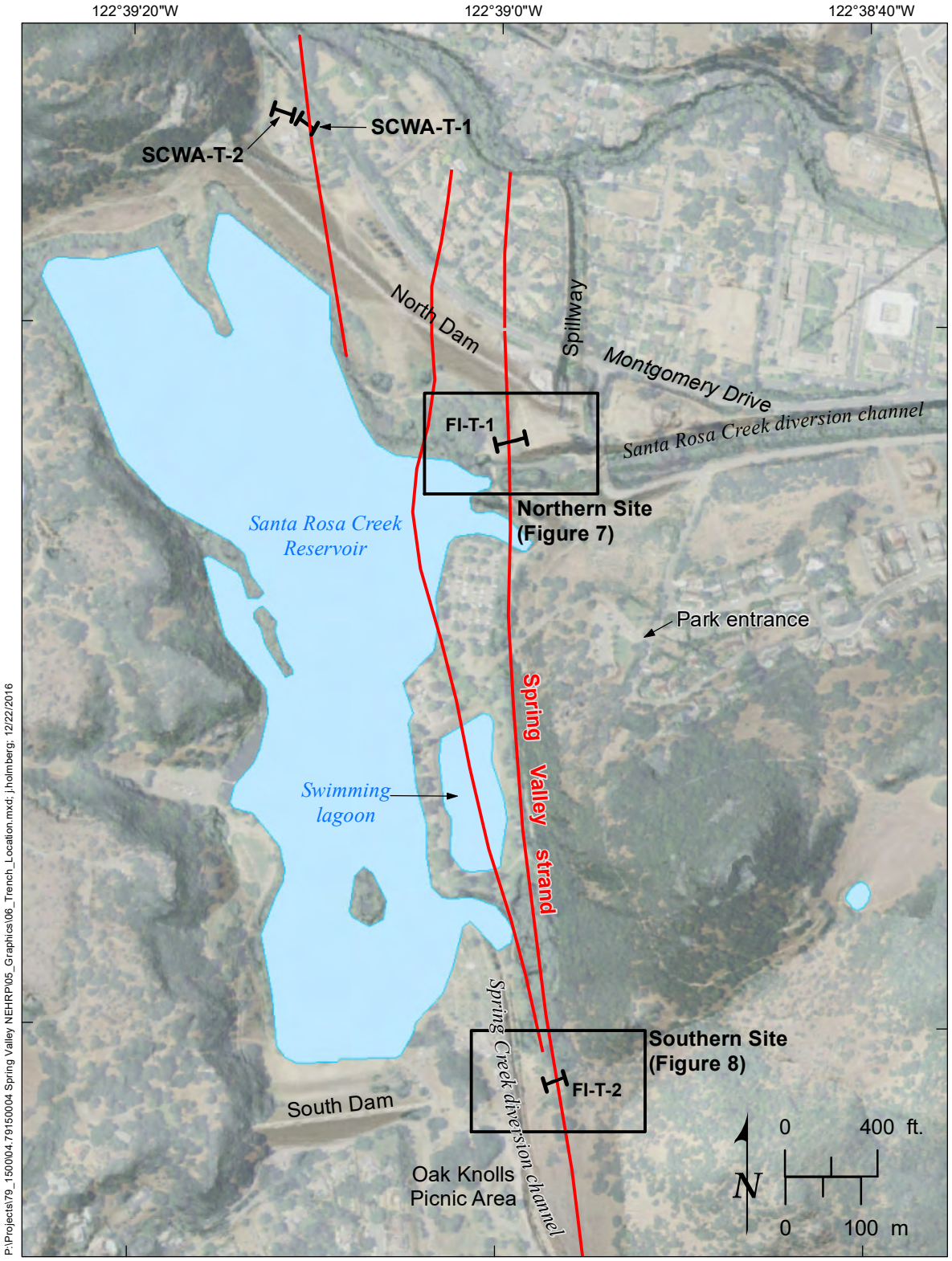

Figure 6. Trench location overview.

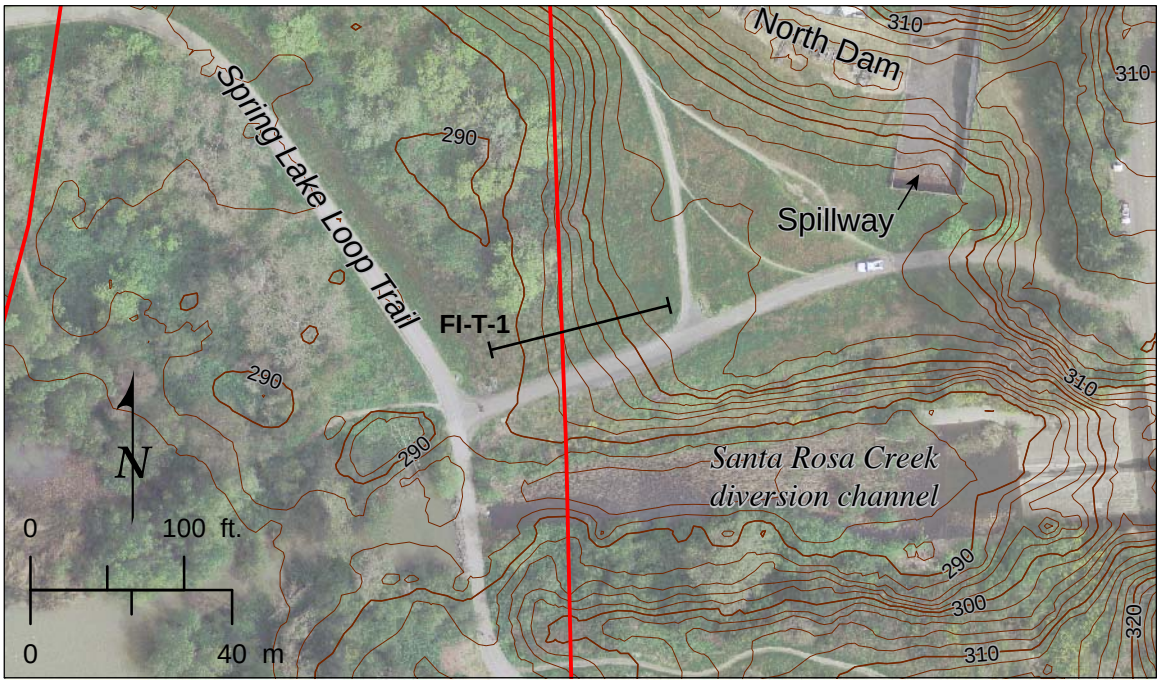

Aerial imagery from USGS, 2011. LiDAR-derived topographic contours from City of Santa Rosa, 2008.

A) Location of Trench FI-T-1 showing mapped fault strands in red.

fwla-wc-file1/Project/Projects/79_1500/04.79150004 Spring Valley NEHRP/05_Graphics

B) View west of excavated and shored Trench FI-T-1.

Figure 7. Location of Trench FI-T-1 at the northern site.

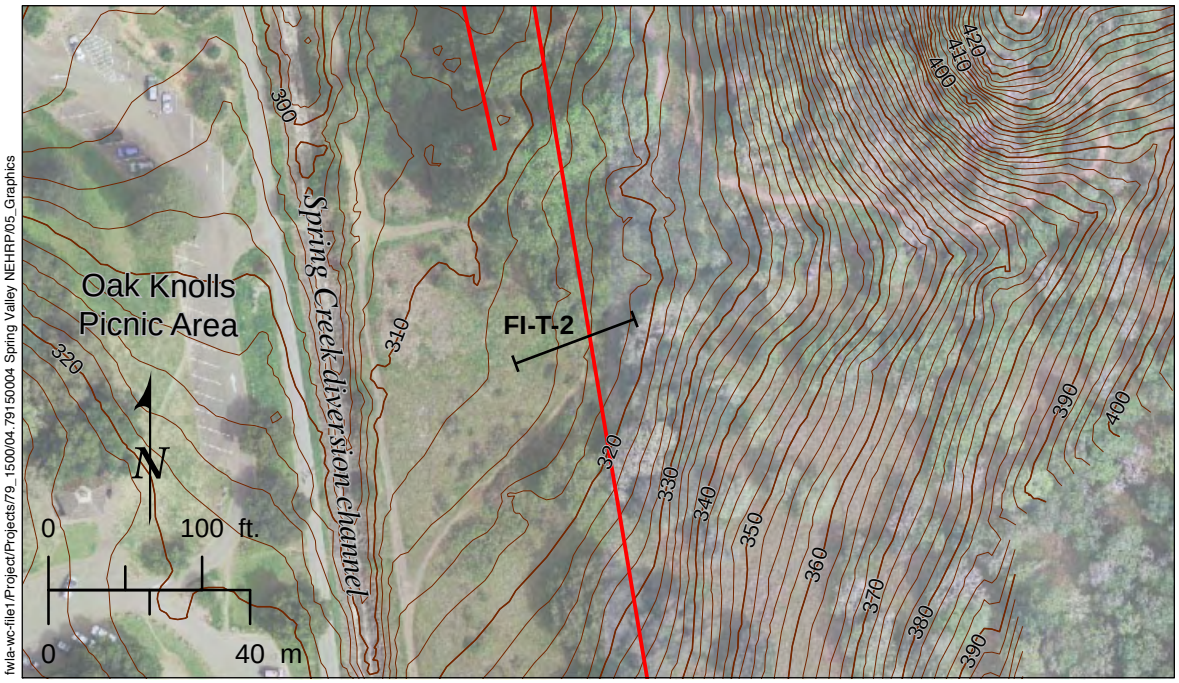

Aerial imagery from USGS, 2011. LiDAR-derived topographic contours from City of Santa Rosa, 2008.

A) Location of Trench FI-T-2 showing mapped fault strands in red.

B) View east of excavated and shored Trench FI-T-2.

Figure 8. Location of Trench FI-T-2 at the southern site.

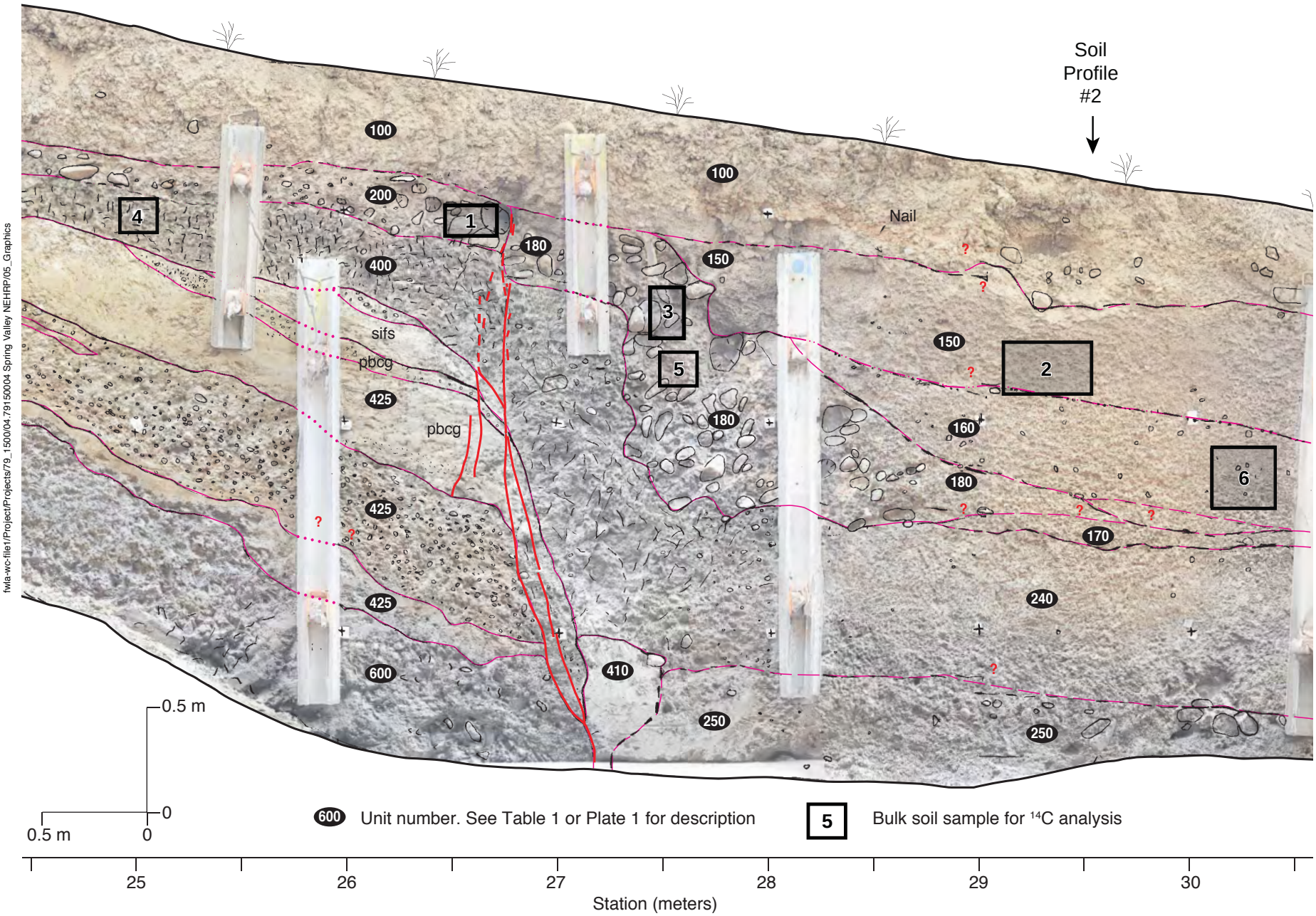

Figure 9. Fault zone detail, Trench FI-T-1.

A) Station 8: Soil Profile 1 location

C) Station 27: Fault flagged in red

B) Station 23: Angular unconformity over dipping alluvium

D) Station 29: Soil Profile 2 location

Figure 10. Photographs of Trench FI-T-1.

EXPLANATION

Symbols

- Soil horizon
- Clear contact/boundary (2.5 to 6 cm)
- Abrupt contact/boundary
- Fault, dashed where approximate
- Mineralization along fracture
- Visible clast
- Absent clast or indentation
- Meter marker
- Sand and fine gravel
- Fractures related to peds and soil desiccation
- Fractures with mineralization (open)
- 3 — Bulk soil sample for 14C analysis

Abbreviations

pbcg	Pebble conglomerate
sifs	Silty fine sand
si	Silt
cl	Clay
apcsfg	Angular pebble coarse sand fault gouge

Unit Descriptions

100 Lean CLAY with Sand and Gravel (CL); Dark yellowish brown 10YR (4/4); 20 to 25% fine to coarse, rounded to subangular sand; 20 to 25% rounded to subrounded gravel; 50 to 60% medium plasticity, medium toughness, no dilatancy fines; stratified to massive; volcanic sands and gravels; A horizon; clay film on clasts; fine roots throughout; gradual lower boundary; Fill

150 Clayey SILT; 2.5Y (3/1); 5% fine to medium, subangular to angular volcanic gravels; 15 to 20% fine to coarse subangular to angular sand; 75 to 80% hard, medium plasticity, low toughness, slow dilatancy, high dry strength fines; no soil structure; common fine pores (1 mm); common fine vertical white roots; clear, wavy lower boundary; A to AB horizon; Colluvial deposit

160 Clayey SILT; 15 to 20% fine to medium, angular to subangular basalt and tuffaceous gravels; 25% fine to coarse, subangular to subrounded sand; 55 to 60% medium plasticity, medium toughness, slow dilatancy, high dry strength fines; common fine pores; rare roots; clear, wavy lower boundary; Bt soil horizon; Colluvial deposit

180a (Unit 170 as it appears in the fault zone) Clayey GRAVEL (GC); Dark brown 10YR (2/2) to very dark grayish brown 10YR (3/2); 30 to 40% coarse, rounded to subangular gravel up to 50 cm; 45 to 55% medium plasticity, medium toughness, no dilatancy fines; 5 to 10% fine to medium sand; grades to finer grained colluvium (unit 170); matrix supported; massive; Bt horizon; clay film on clasts; vertically oriented gravels near fault plane; fine roots throughout; clasts are heavily weathered; wavy, gradational lower contact; Colluvial deposit

180 Silty CLAY; 2.5Y (3/1); <5% fine to medium, subangular to subrounded gravel; 5 to 10% fine to medium sand; 85 to 90% medium plasticity, medium toughness, slow dilatancy, high dry strength fines; massive; non-weathered; weak columnar to blocky peds; rare fine pores; rare fine roots; no clay film on clasts; gradual, smooth to wavy lower boundary; distal portion of Colluvial deposit

200 Sandy Lean CLAY with Gravel (CL); Dark yellowish brown 10YR (3/4); 15% subrounded to subangular gravels; 20 to 30% fine to coarse, moderately graded, rounded to subangular sand; 55 to 65% medium plasticity, medium toughness, no dilatancy fines; volcanic sands and gravels up to 13 cm; stratified to massive; A-B horizon; granular; minor clay film on clasts; clear lower boundary; fine roots throughout; gravels are confined to lower 8 to 10 cm of unit; possibly Fill or disturbed Fluvial deposit (plow zone)

240 Clayey SILT with Sand and Gravel; 2.5Y (4/2); 5% subrounded to rounded cobbles; 10 to 15% fine to coarse, subangular to angular gravels; 5 to 10% medium to coarse subangular sand; 70 to 80% high plasticity, medium toughness, slow dilatancy, medium dry strength fines; massive; no soil structure; rare fine roots; gradual, wavy lower boundary; Colluvial deposit

250 Lean CLAY with Sand and Gravel (CL); Olive-brown 2.5Y (4/3); soft; wet; 10 to 15% fine to medium sand; 10 to 15% coarse, rounded to subrounded gravel up to 17 cm; 70 to 80% medium plasticity, medium toughness, no dilatancy fines; massive; rare to no roots; Bt horizon; moderately to heavily weathered volcanic sand and gravel; Colluvial deposit

300 Clayey SAND with Gravel (SC); Dark brown 7.5YR (3/3); 20% subrounded to subangular gravel up to 6 to 8 cm; 30% medium plasticity, medium toughness, no dilatancy fines; 50% well-graded, fine to coarse, subrounded to angular sand; volcanic sands and gravels; stratified; Bt horizon; blocky to granular; fine roots in places; clay film on clasts; clasts are heavily weathered; lenses of fine sand are defining feature of unit, typically 6 to 8 cm thick; Fluvial deposit

400 (Unit description done at station 14.5) Lean CLAY with Sand and trace Gravel (CL); 5% medium, subangular to subrounded gravel; 10 to 15% fine to coarse, poorly graded, angular to subangular sand; 80 to 85% medium plasticity, medium toughness, no dilatancy fines; blocky; massive; volcanic lithics; sharp erosional lower contact; fine roots throughout; Fluvial deposit

405 Lean CLAY (CL); Olive-brown 2.5Y (4/3); 98 to 100% medium toughness, medium plasticity, no dilatancy fines; <2% trace fine sand; stratified; Bt horizon; blocky; fine roots throughout; waxy texture on pedogenic faces; wavy, clear lower boundary; Fluvial deposit

410 Lean CLAY with SILT (CL); Olive 5Y (5/3); soft, gouge material; wet; 95 to 100% medium toughness, medium plasticity, slow to no dilatancy fines; up to 5% fine sand; massive; Bt horizon?; gradational lower contact; Fault gouge

425 (Fluvial package truncated by fault) SILT with fine Sand (ML) interfingered with Clayey SAND (SC); Olive-brown 2.5Y (4/3) to Dark yellowish brown 10YR (4/4); upper and lower silt with fine sand packages consist of: 40 to 50% fine sand; 50 to 60% fines; stratified to massive; granular; wavy to irregular lower contact along lower silt package with heavy iron oxide staining; wavy lower contact with little to no iron oxide staining along upper silt package; interfingered clayey sand consist of: 5 to 15% rounded to subrounded gravel; 15% medium plasticity, medium toughness, no dilatancy fines; 70 to 80% poorly graded, fine to coarse, rounded to subangular sand; volcanic clasts; wavy lower contact; iron oxide staining along lower 17 to 25 cm of unit; stratified to massive; Fluvial deposit

450 (Fluvial channel deposit, west side of trench) Clayey SAND with Gravel (SC); Dark yellowish brown 10YR (4/4); 20% subrounded to subangular gravel; 30% medium plasticity, medium toughness, no dilatancy fines; 50% fine to coarse, rounded to angular sand; volcanic and sedimentary clasts; stratified; Bt horizon; blocky to granular; clay film on clasts; clasts are heavily weathered; thin lenses of sand present in unit 300 are absent; clear, wavy lower contact; Fluvial deposit

500 Lean CLAY (CL); Olive-brown 2.5Y (4/3); 98 to 100% medium toughness, medium plasticity, no dilatancy fines; 0 to 2% trace fine to medium sand; stratified; Bt horizon; blocky; fractures with silica? mineralization along fracture planes; waxy texture along pedogenic faces; wavy, clear lower boundary up to 2.5 cm; fine roots throughout; Fluvial deposit

600 Lean CLAY with Sand with interbeds to lenses of Poorly Graded SAND with clay (CL to SP); Olive-brown 2.5Y (4/3); 40 to 50% medium toughness, medium plasticity, no dilatancy fines; 50 to 60% fine to coarse, subrounded to subangular sand; granite, quartz, basalt, chert and other volcanic lithics up to 1 cm diameter; trace gravels up to 5 to 7 cm; lenses of sand and gravel are up to 8 inches thick with iron oxide and manganese staining in places; stratified; Bt horizon; blocky; clay film and waxy surfaces on lithics; clasts are heavily weathered; Fluvial deposit

Plate 1. Photographic and geologic logs of Trench FI-T-1.

Photographic Log, Trench FI-T-2

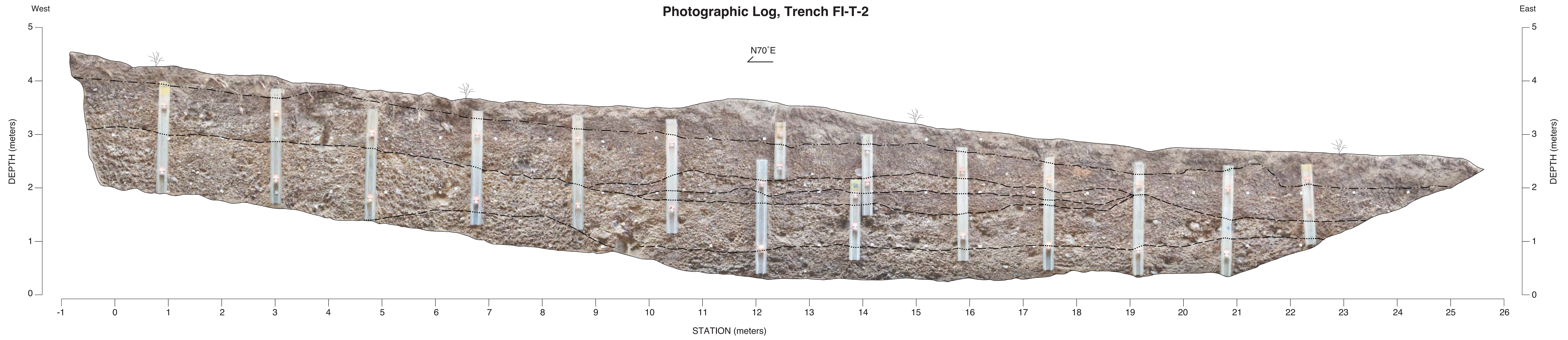

Geologic Log, Trench FI-T-2

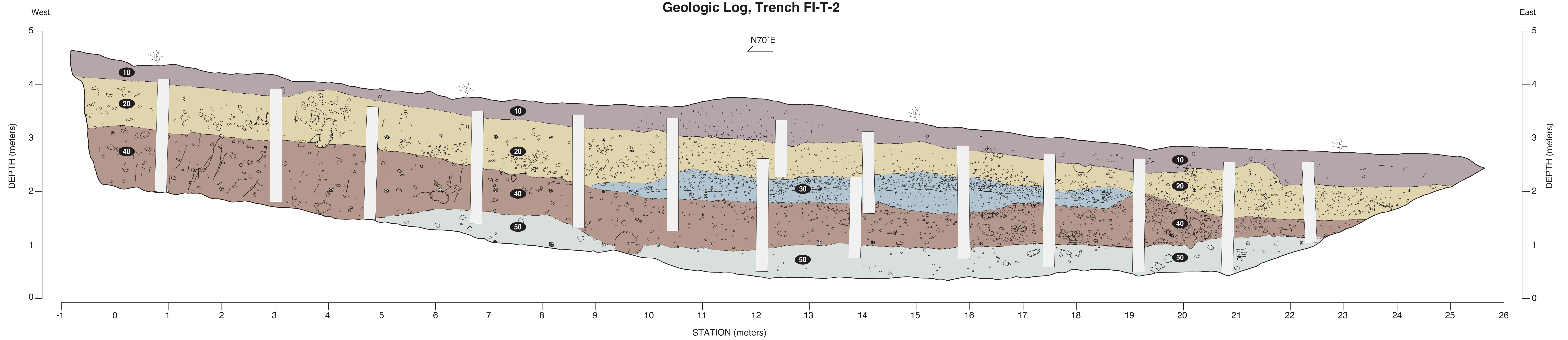

EXPLANATION

Symbols

- Root
- Blocky pedogenic structure
- Soil horizon
- Clear contact/boundary (2.5 to 6 cm)
- Abrupt contact/boundary
- Visible clast
- Absent clast or indentation
- Meter marker
- Sand and fine gravel
- Fractures related to shrinking and swelling of clays

Unit Descriptions

10 Lean CLAY with Sand and trace Gravel (ML); 5% coarse, subrounded volcanic gravels; 30% fine to medium sand; 65% medium toughness, medium plasticity fines; massive; A horizon; minor clay on clasts; Fill?

20 Sandy Lean CLAY with SILT (CL); Dark Brown 7.5YR (3/3); 30-40% fine to coarse, poorly graded, subrounded to subangular volcanic sands; 60-70% medium plasticity, medium toughness fines; A-B horizon; massive to blocky; fine roots throughout; Colluvium

30 Sandy Lean CLAY with Gravel (CL); Dark Brown 7.5YR (3/3); 10-20% medium, subangular to subrounded gravel up to 15-cm; 30-40% medium plasticity, medium toughness fines; 40-50% fine to coarse, poorly graded, subrounded to subangular sand; massive; Bt horizon; volcanic lithics; heavily weathered clasts; fine roots throughout; Colluvium

40 Sandy SILT with Gravel (ML); Brown 7.5YR (4/3); 20% coarse, subangular to subrounded gravel; 30% low plasticity, low toughness fines; 50% fine to coarse, poorly graded sand; massive; volcanic lithics; gravel up to 15-cm; fine roots throughout; root casts in places; Colluvium

50 SILT with Sand and Clay (ML); Dark Brown 7.5YR (3/3); 30-40% fine sand; 60-70% low plasticity, low toughness, slow dilatancy fines; massive; Bt horizon; rare coarse, subangular volcanic gravel up to 5-cm; minor clay film on gravels; Colluvium

Paleoseismic investigation of the Spring Valley strand of the Bennett Valley Fault, Santa Rosa, California.
Draft November 10, 2016 Final Technical Report.

Plate 2. Photographic and geologic logs of Trench FI-T-2.

Photographic Log, SCWA-T-1

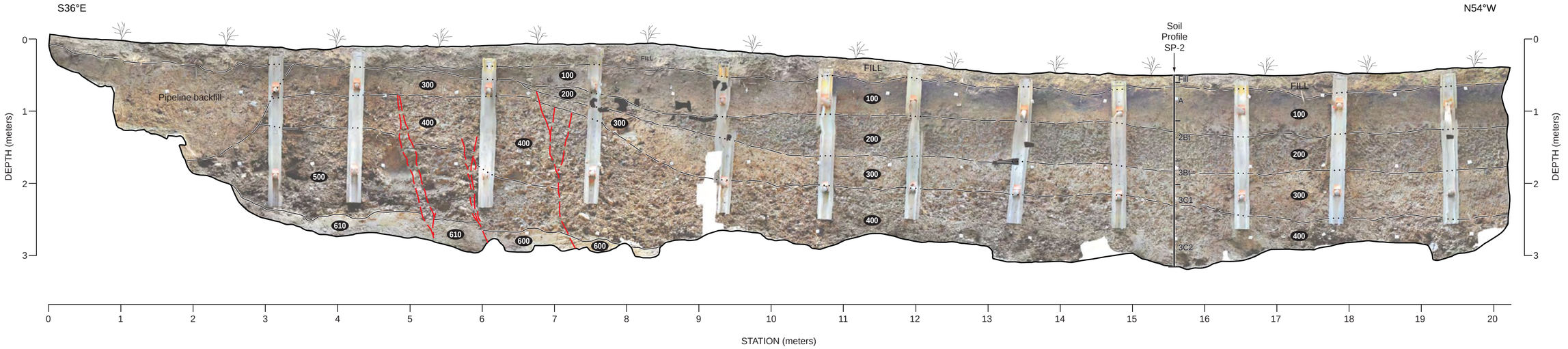

Geologic Log, SCWA-T-1

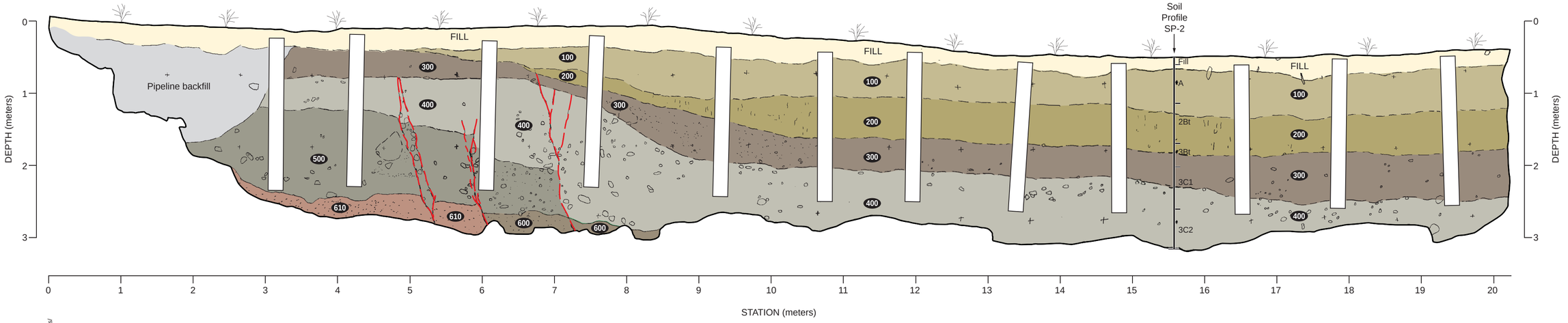

I:\ata-wc-file1\project\Projects\79_1500\04-79150004 Spring Valley NEH\RPT\05_Graphics\

EXPLANATION

Symbols

- Clear contact/boundary (2.5 to 6 cm)
- Abrupt contact/boundary
- Fault, dashed where approximate

Unit Descriptions

100 SILT with clay (ML), dark reddish brown 5YR (2.5/2) to very dark brown 10YR (2/2); massive; 0 to 2% coarse gravel; sub-rounded, volcanic; 98 to 100%, damp, low plasticity, soft, no dilatancy fines.

200 Base of brown clay in T-1 and T-2; CLAY (CL) with fine sand; dark reddish brown 5YR (2.5/2) to very dark brown 10YR (2/2); massive; 0 to 5% coarse gravel, sub-rounded to sub-angular, primarily Sonoma Volcanics; 5 to 10% fine, sub-rounded to sub-angular sand; 80 to 90% low to medium plasticity; damp (moisture decreases with depth), stiff, no dilatancy fines; soil ped structures apparent where moisture content is lower.

300 Clayey SAND (SC) with some coarse gravel; brown 7.5YR (4/4) to dark yellowish brown 10YR (3/6); 0 to 10% sub-rounded to sub-angular coarse gravel, generally weathered, primarily andesites and basalt (Sonoma volcanics); 10-20%, low plasticity, dry, hard, no dilatancy fines; 70 to 80% fine to medium, sub-angular to sub-rounded sand, indurated where dry, can form ped-like structures.

400 Clayey GRAVEL (GC); dark brown 7.5YR to 10YR (3/3); 20% rounded to sub-rounded gravel, clasts up to 23 cm, basalts and andesites (Sonoma Volcanics), clay films on some clasts; clasts heavily weathered; 30 to 40% medium plasticity, moist, soft, no dilatancy fines; 50% fine to coarse, sub-angular to rounded sand, fines upwards; In T-2 gravel continues to trench floor at least 1 m thick; in T-2 several units are apparent beneath the gravel

500 Clayey GRAVEL (GC); dark brown 7.5YR to 10YR (3/3); 20 to 30% medium plasticity, moist, soft, no dilatancy fines; 30% rounded to sub-rounded gravel, cobbles up to approximately 30 cm, basalts and andesites (Sonoma Volcanics), clay films on some clasts; clasts heavily weathered; 40% fine to coarse, sub-angular to rounded sand.

600 SILT (ML) with some sand; pale yellow 2.5YR (7/4) to light yellowish brown 2.5YR (6/4); <5% coarse, sub-rounded to sub-angular sand, up to 4 mm; 95% low plasticity, damp, soft, no dilatancy fines; thin brownish clay coating visible where roots are present.

610 CLAY with silt (CL); reddish brown 5YR (4/4) to brown 7.5YR (4/4); <1% sub-rounded to sub-angular gravel, up to 2 cm, basalt (Sonoma Volcanics); 99 to 100% low to medium plasticity, moist, soft, no dilatancy fines.

Plate 3. Photographic and geologic logs of Trench SCWA-T-1.

APPENDIX A

PaleoResearch Institute

Radiocarbon Report

EXAMINATION OF BULK SOIL, MICROCHARCOAL EXTRACTION, AND AMS RADIOCARBON AGE DETERMINATION FOR THE NORTH TRENCH OF THE SPRING VALLEY PALEOSEISMIC INVESTIGATION, SONOMA COUNTY, CALIFORNIA

By

Peter Kováčik

With assistance from
R. A. Varney

PaleoResearch Institute, Inc.
Golden, Colorado

PaleoResearch Institute Technical Report 2016-032 and 2016-092

Prepared for

Fugro Consultants, Inc.
Walnut Creek, California
and
Earthquake Science Center, USGS
Menlo Park, California

December 2016

INTRODUCTION

The North Trench of Spring Valley Paleoseismic Investigation is located in Spring Lake Park within the city of Santa Rosa in Sonoma County, California (Janet Sowers, personal communication March 11, 2016). Six bulk soil samples collected from five different units were submitted for macrofloral analysis to recover charred remains suitable for AMS radiocarbon analysis. In addition, microscopic charcoal recovery was requested for three of these sediments. Charred remains from three samples and three microcharcoal samples were submitted for AMS radiocarbon age determination.

METHODS

Macrofloral

Bulk samples were floated using a modification of procedures outlined by Matthews (1979). Each sample was added to approximately three gallons of water, then stirred until a strong vortex formed. The floating material (light fraction) was poured through a 250-micron mesh sieve. All material that passed through the screen was retained for possible microcharcoal, particulate soil organics, and/or humate extraction. Additional water was added and the process repeated until all floating material was removed from the samples (a minimum of five times). The material remaining in the bottom (heavy fraction) was poured through a 0.5-mm mesh screen. The floated portions were allowed to dry.

The light fractions were weighed, then passed through a series of graduated screens (US Standard Sieves with 4-mm, 2-mm, 1-mm, 0.5-mm, and 0.25-mm openings) to separate charcoal debris and to initially sort the remains. Contents of each screen then were examined. Charcoal pieces larger than 1 mm, 0.5 mm, 0.25 mm in diameter were separated from the rest of the light fraction, and the total charcoal was weighed. Charcoal pieces in a representative sample were broken to expose fresh cross, radial, and tangential sections, then examined under a binocular microscope at a magnification of 70x and under a Nikon Optiphot 66 microscope at magnifications of 320–800x. Weights of each charcoal type within the representative sample were recorded. Material that remained in the 4-mm, 2-mm, 1-mm, 0.5-mm, and 0.25-mm sieves was scanned under a binocular stereo microscope at a magnification of 10x, with some identifications requiring magnifications of up to 70x. Material that passed through the 0.25-mm screen was not examined. Heavy fractions were scanned at a magnification of 2x for the presence of botanic remains. The term "seed" is used to represent seeds, achenes, caryopses, and other disseminules. Remains from the light and heavy fractions were recorded as charred and/or uncharred, whole and/or fragments. Macrofloral remains, including charcoal, were identified using manuals (Carlquist 2001; Hoadley 1990; Martin and Barkley 1961; Musil 1963; Schopmeyer 1974; Schweingruber et al. 2011, 2013) and by comparison with modern and archaeological references. Clean laboratory conditions were used during flotation and identification to avoid contamination of charcoal and botanic remains to be submitted for radiocarbon dating. All instruments were washed between samples, and the samples were protected from contact with modern charcoal.

AMS Radiocarbon Dating - Charcoal and Microcharcoal

Charred botanic and charcoal samples submitted for radiocarbon dating were identified and weighed prior to selecting subsamples for pre-treatment. The remainder of each subsample that proceeds to pre-treatment, if any, is curated permanently at PaleoResearch Institute. Selected subsamples were vacuum freeze-dried, freezing out all moisture at -107 °C and < 10 millitorr. Then samples were treated with cold pH 2 hydrochloric acid (HCl), followed by cold 6N HCl. Samples then were heated to approximately 110 °C while in 6N HCl. This step was repeated until the supernatant was clear. This step removes iron compounds and calcium carbonates that hamper humate compound removal. Next, the samples were subjected to dilute 0.05% potassium hydroxide (KOH) to remove humates using both cold solutions and solutions that were heated. Once again, the samples were rinsed to neutral and re-acidified with pH 2 HCl between each KOH step. This step was repeated until the supernatant was clear, signaling removal of all humates, then was rinsed to neutral. After humate removal, samples were made slightly acidic with pH2 HCl. Each sample was freeze-dried, then combined in a quartz tube with a specific ratio of cupric oxide (CuO) and elemental silver (Ag) in quantities based on the mass of carbon in the sample. The tubes were hydrogen flame-sealed under vacuum.

The bulk soil samples were floated and screened through 250-micron (µ) mesh to recover charcoal for AMS radiocarbon dating. Sediment and organics that passed through the sieve were retained in case insufficient macroscopic charcoal was recovered. Recovery of microscopic charcoal and particulate soil organics from sediments using heavy liquid extraction yields materials that may be subjected to the same chemical pre-treatment used on larger pieces of charcoal prior to radiocarbon age determination. This technique, complete with acid and base chemistry, yields ages comparable to those obtained on charcoal, rather than resembling soluble organic (humate) dating.

Microscopic charcoal is too small for identification. Hydrochloric (HCl) acid (10%) was added to the samples to remove calcium carbonates. Samples were rinsed until neutral, and a small quantity of sodium hexametaphosphate was added to begin clay removal. The samples' beakers were filled with reverse osmosis deionized (RODI) water and allowed to settle according to Stoke's Law. After two hours the supernatant, containing clay, was poured off and the samples were rinsed with RODI water three more times, each time being allowed to settle according to Stoke's Law to remove more clays. This sequence was repeated, as necessary, to remove clays.

After clay removal, the samples were freeze-dried. Sodium polytungstate (SPT) with a density of 2.1 was used for the flotation process. The dry samples were mixed with SPT and centrifuged at 1,500 rpm for 10 minutes to separate organic from inorganic remains. The supernatant containing pollen, organic remains, and microscopic charcoal was decanted. Sodium polytungstate was added to the inorganic fraction to repeat the separation process until all organic material was collected (usually three repetitions). Microscopic charcoal fragments were separated from the SPT by diluting this mixture with RODI water and centrifuging, after which each sample was rinsed thoroughly with RODI water. Following this step, a 25 to 120 minute hydrofluoric acid (HF) treatment dissolved residual silicate minerals. Samples were rinsed with RODI water to neutrality. Hydrofluoric acid treatments were repeated, if necessary, until examination of the samples using a binocular microscope indicated only organics remained, including microcharcoal. Following this step, a small quantity of hot concentrated

nitric acid was added to the samples' tubes, which were placed in hot sand for approximately 120 minutes. Nitric acid is used to oxidize and remove uncharred particulate organics. Following nitric acid treatment, the samples were rinsed copiously with RODI water and vacuum dried.

This resulting mixture of charcoal and particulate soil organics then was subjected to the rigorous acid-base-acid chemical pre-treatment required prior to radiocarbon dating. Six normal (6N) hydrochloric acid was added to remove iron and any residual carbonates from the samples. This step was repeated until the solution was clear and colorless. For these samples, one (PRI-5536 and PRI-5537) and three (PRI-5364) rinses in 6N were required to complete iron removal before they were rinsed to neutrality with RODI water. Dilute potassium hydroxide (0.05% KOH) was added to the samples and heated to 100°C to remove humates and related soluble organic contamination. KOH treatment was repeated at one (PRI-5536 and PRI-5537) to three (PRI-5364) times until the solution was clear and colorless, indicating organic contaminant removal. Samples were then rinsed to neutrality with RODI water, vacuum dried, and examined using a stereoscope to verify organic removal and assess the quality of the remaining microscopic charcoal. The samples were vacuum dried, then reexamined using a binocular microscope at a magnification of up to 30x to check for charcoal and particulate organic presence. Finally, samples were freeze-dried, then combined in a quartz tube with a specific ratio of cupric oxide (CuO) and elemental silver (Ag) in quantities based on the mass of carbon in the sample. The tubes were flame-sealed under vacuum.

Standards and laboratory background wood samples were treated to the same acid and base processing as wood and charcoal samples of unknown. A radiocarbon "dead" wood blank from the Gray Fossil site in Washington County, Tennessee, dated to the Hemphillian stage of the late Miocene, 4.5-7 MYA (currently beyond the detection capabilities of AMS) was used to calibrate the laboratory correction factor. In addition, standards of known age, such as the Third International Radiocarbon Inter-comparison (TIRI) Sample "B" (Belfast Pine) with a consensus age of 4503 ± 6, and TIRI Sample "J" (Bulston Crannog wood) with a consensus age of 1605 ± 8 (Gulliksen and Scott 1995), are used to help establish the laboratory correction factor. After the requisite pre-treatment, a quantity similar to submitted samples of each wood standard was sealed in a quartz tube. Once all the wood standards, blanks, and submitted samples of unknown age were prepared and sealed in their individual quartz tubes, they were combusted at 820 °C, soaked for an extended period of time at that temperature, and allowed to cool slowly, enabling the chemical reaction that extracts carbon dioxide (CO_2) gas.

Following this last step, all samples of unknown age, the wood standards, and the laboratory backgrounds were sent to The Center for Applied Isotope Studies in Athens (CAIS), Georgia, where the CO_2 gas was processed into graphite. The graphitized samples were placed in the target and run through the accelerator, generating numbers that are subsequently converted into radiocarbon dates. Data presented in the discussion section are displayed as conventional radiocarbon ages and calibrated ages using IntCal13 curves on OxCal version 4.2.4 (Bronk Ramsey and Lee 2013; Bronk Ramsey 2009; Reimer et al. 2013). This probability-based method for determining conventional ages provides a calibrated date reflecting the probability of its occurrence within a given distribution (signaled by the amplitude [height] of the curve). This method is different from the intercept-based method of individual point estimates that provides no information concerning probabilities. As a result, the probability-based method offers more stability to the calibrated values than those derived from intercept-based methods, which are subject to adjustments in the calibration curve (Telford et al. 2004).

RADIOCARBON REVIEW

Radiocarbon dates from non-annuals, such as trees and shrubs, reflect the age of that portion of the tree/shrub when it stopped exchanging carbon with the atmosphere, not necessarily the date the tree/shrub died or was burned. Trees and shrubs grow each year by adding new layers or rings of cells to the cambium. During photosynthesis, new cells take in atmospheric carbon dioxide, which includes carbon-14 (^{14}C) or radiocarbon. The radiocarbon absorbed is consistent with atmospheric ^{14}C levels during that growth season. Metabolic processes stop for the inner sapwood once it is converted into heartwood. At this point, no new carbon atoms are acquired, and the radiocarbon that is present starts to decay. Studies show there is little to no movement of carbon-bearing material between rings (Berger 1970, 1972 in Taylor and Bar-Yosef 2014:67). As a result, wood from different parts of the tree yields different radiocarbon dates (Puseman 2007). The outer rings exhibit an age close to the cutting or death date of the tree, while the inner rings reflect an early stage of tree growth. Because the younger, outer rings burn to ash first, usually it is the older, inner rings that are remaining in a charcoal assemblage (Puseman et al. 2009; Taylor 1987).

Radiocarbon age calibrations are based on comparisons between measured ^{14}C and calendar dates determined by dendrochronology and other techniques. The relationship between measured ^{14}C ages and calendar dates is not a straight line, but instead includes fluctuations. A “squiggly” line from the upper left toward the lower right portion of the calibration figure depicts these fluctuations, which have their basis in variability in the ratio of ^{14}C present in the atmosphere through time, among other things. The elongated bell-shaped curve at the left margin of the calibration window depicts the two-sigma probability range (± values) around a central point (radiocarbon date in RCYBP) (Taylor and Bar-Yosef 2014:156-157). The solid black peaks at the bottom of the graph represent the intersection of the bell-shaped curve and the “squiggly” line of the calibration curve. Their amplitude and area of coverage indicate the probability that the radiocarbon date falls within any given year range. Brackets along the bottom edge of these peaks indicate the one-sigma and two-sigma ranges. These probabilities also are presented at the right side of the figure. The probability does not provide a value judgment or measure of the appropriateness for any point on the calibration curve. In contrast, an intercept date represents the central point between the two extremes of the calibrated age range. This intercept point or mathematical central point may fall in a zero probability portion of the calibration curve. Additional information from samples’ proveniences and their contexts relative to architectural features, such as collapsed walls or capped features, facilitates evaluation and interpretation of which calibrated date range portions most accurately represent occupation or the activity of interest.

DISCUSSION

Situated near the Spring Lake Reservoir in Santa Rosa, Sonoma County, California, the North Trench exposure displayed fluvial sediments from Santa Rosa Creek. The site lies on a grassy slope within Spring Lake Park. Grading that occurred in the area in the 1960s during dam construction resulted in one to two feet of fill accumulation over the slope. Local vegetation consists of valley oak (*Quercus lobata*), coast oak (*Quercus parvula*), coyote bush

(*Baccharis pilularis*), California laurel (*Umbellularia californica*), California buckeye (*Aesculus californica*), and redwood (*Sequoia sempervirens*). Invasive species include eucalyptus (*Eucalyptus*) (Janet Sowers, personal communication March 11, 2016). Macrofloral remains, including charcoal recovered in six bulk soil samples from the North Trench site, were identified, and charred remains appropriate for AMS radiocarbon analysis were isolated. Microscopic charcoal was recovered from three sample. Three charcoal samples and three microscopic charcoal samples were selected for AMS radiocarbon age determination (Table 1).

Collected from a colluvial deposit (Unit 160) at a depth of 1.19 mbs (1.5 mad), Bulk Sample 6 contained numerous uncharred rootlets and 11 tiny (~0.25 mm) unidentifiable charcoal fragments (Tables 2 and 3) weighing less than 0.0001 g. Identification to species was not possible due to size and level of vitrification of the material. Vitrified charcoal has a shiny, glassy appearance that can range from still recognizable in structure "to a dense mass, completely 'molten' and non-determinable" (Marguerie and Hunot 2007; McParland et al. 2010). Although charcoal vitrification has been attributed to burning at high temperature and/or burning green wood, the process of vitrification is not completely understood. Experimental studies and reflectance measurements on archaeological charcoal suggest that vitrification can occur at low temperatures (McParland, et al. 2010). Kaelin et al. (2006:1-12) associate vitrification with changes in the lignin structure of wood. Specifically, they implicate changes resulting from "reactions involving and altering the nature of the C3 side-chain unit, reducing the number of β-O-4 linked lignin units" (Kaelin, et al. 2006:10). Experiments examining wood composition changes during heating at low and high temperatures (Rutherford et al. 2005) indicate transformation of lignin, identified using Fourier Transform Infrared (FTIR) analysis. Although charcoal fragments recovered in this sample are not sufficient for AMS radiocarbon analysis (less than 0.0001 g), their presence indicates the potential for this sample to contain charred microscopic fragments (microscopic charcoal). Microscopic charcoal can be extracted from the sediment that passed through the 250-micron-mesh sieve during the flotation procedure and has been retained. Recovery of charred macroscopic remains in sufficient mass for AMS radiocarbon dating from geological samples is often very limited. Retention of sediments for possible microscopic charcoal, particulate soil organics, and/or humate extraction is part of our policy to provide additional options when sediments yield insufficient mass or lack any macroscopic charred remains for AMS radiocarbon dating. Retained sediments from Sample 6 were selected by the client and processed at PRI to recover microscopic charcoal. Successful extraction yielded a mass sufficient (0.0819 g) for AMS radiocarbon age determination. A date of 4192 ± 24 RCYBP (PRI-5536) with two-sigma calibrated age ranges of 4840–4790 and 4770–4620 CAL yr. BP (Table 4 and Figure 1) was obtained.

Sample 5, collected from Unit 180 (distal portion of colluvial deposits) at a depth of 1.14 mbs (2.1 mad), yielded numerous uncharred rootlets and 18 unidentifiable charcoal fragments (0.0007 g), too small and too vitrified for identification. Microscopic charcoal extracted from retained sediments yielded a date of 2830 ± 24 RCYBP (PRI-5364). This date calibrates to an age range of 3000–2860 CAL yr. BP (Figure 2) at the two-sigma level, indicating Unit 180 deposits are younger than those from Unit 160 (Figure 3).

Another sample (3) from Unit 180 was collected at a depth fo 1.14 mbs (2.5 mad). Sample 3 yielded numerous uncharred rootlets and 14 small (~0.25 mm) and vitrified, unidentifiable charcoal fragments (0.0012 g). These fragments were submitted for radiocarbon analysis returning a date of 1662 ± 29 RCYBP (PRI-5535) and two-sigma calibrated age ranges of 1690–1670, 1630–1520, 1460–1440, and 1430–1420 CAL yr. BP (Figure 4).

Fluvial deposits (Unit 400) sampled (Sample 4) at a depth of 0.81 mbs (3 mad) contained numerous rootlets and a few uncharred sclerotia. Sclerotia are commonly called "carbon balls." They are small, black, solid or hollow spheres that can be smooth or lightly sculpted. These forms range from 0.5 to 4 mm in size. Sclerotia are commonly called "carbon balls." They are small, black, solid or hollow spheres that can be smooth or lightly sculpted. These forms range from 0.5 to 4 mm in size. Sclerotia are the resting structures of mycorrhizae fungi, such as *Cenococcum graniforme*, that have a mutualistic relationship with tree roots. Many trees are noted to depend heavily on mycorrhizae and might not be successful without them. "The mycelial strands of these fungi grow into the roots and take some of the sugary compounds produced by the tree during photosynthesis. However, mycorrhizal fungi benefit the tree because they take in minerals from the soil, which are then used by the tree" (Kricher and Morrison 1988:285). Sclerotia appear to be ubiquitous and are found with coniferous and deciduous trees including *Abies* (fir), *Juniperus communis* (common juniper), *Larix* (larch), *Picea* (spruce), *Pinus* (pine), *Pseudotsuga* (Douglas fir), *Alnus* (alder), *Betula* (birch), *Populus* (poplar, cottonwood, aspen), *Quercus* (oak), and *Salix* (willow). These forms originally were identified by Dr. Kristiina Vogt, Professor of Ecology in the School of Forestry and Environmental Studies at Yale University (McWeeney 1989:229-230; Trappe 1962). The charcoal assemblage consists of two incompletely charred and compressed conifer charcoal fragments (0.0002 g) and four unidentifiable charcoal fragments (0.0001 g), reflecting unspecified conifer and possibly other wood types. Even if combined, these charcoal fragments are not large enough for radiocarbon analysis. The client requested microscopic charcoal extraction and subsequent AMS radiocarbon analysis for this sample. The extracted microscopic charcoal provided the oldest date for this project, 6115 ± 25 RCYBP (PRI-5537), with calibrated age ranges of 7160–7050 and 7030–6890 CAL yr. BP (Figure 5) at the two-sigma level.

Bulk soil (Sample 2) was removed from Unit 150, a colluvial deposit with clayey sediments, at a depth of 0.79 mbs (2.2 mad). This sample yielded various charred floral remains including an awn (0.0001 g), a monocot/herbaceous dicot stem (0.0002 g), a single piece of parenchymous tissue (0.0005 g), and four vitrified tissue fragments. Parenchyma is the botanical term for relatively undifferentiated tissue composed of many similar cells with thin primary walls. Parenchyma occurs in many different plant tissues in varying amounts, especially large fleshy organs such as roots and stems, but also in fruits, seeds, cones, periderm (bark), leaves, needles, etc. (Hather 2000:1; Mauseth 1988). A single *Quercus* charcoal fragment (0.0039 g) and two unidentified hardwood charcoal fragments (0.0002 g) also were recovered, indicating burned oak and possibly other hardwood. Oak charcoal was selected for AMS radiocarbon age determination, yielding a date of 2178 ± 23 RCYBP (PRI-5363). This date calibrates at the two-sigma level to age ranges of 2310–2220 and 2210–2120 CAL yr. BP (Figure 6). Uncharred floral remains noted in Sample 2 include a few *Calandrinia* (calandrinia/red maids), a single Caryophyllaceae seed fragment (a member of the pink family), and numerous rootlets.

Unit 200 represents possible fill or disturbed fluvial deposits (plow zone). Sample 1, collected from this unit at a depth of 0.58 mbs (3.0 mad), contained uncharred roots/rootelts and sclerotia. The charcoal record yielded 30 unidentifiable charcoal fragments (0.0022 g), too small and too vitrified for further identification. A date of 399 ± 27 RCYBP (PRI-5534) with two-sigma calibrated age ranges of 520–420 and 380–320 CAL yr. BP (Figure 7) was produced.

SUMMARY AND CONCLUSIONS

Examination of six sediment soil samples from different deposits at the North Trench, Spring Valley Paleoseismic Investigation in Santa Rosa, Sonoma County, California, resulted in recovery of few charred floral remains and small charcoal fragments, some in sufficient quantities for AMS radiocarbon age determination.

Charcoal recovered in these deposits include unspecified conifer, oak (Sample 2), and possibly other hardwoods, reflecting local trees or shrubs that burned in local wildfires. Sample 2 also yielded burned monocots (grasses/sedges) or non-woody members of the Dicotyledonae class. A charred awn fragment may reflect grasses or storksbill/filaree. In addition, single charred parenchymous tissue and vitrified tissue fragments also were noted.

The oldest dates (Figure 3): 6115 ± 25 RCYBP (PRI-5537), 4192 ± 24 RCYBP (PRI-5536), and 2830 ± 24 RCYBP (PRI-5364), were obtained on microscopic charcoal extracted from retained floatation sediments from Samples 4 (Unit 400), 6 (Unit 160), and 5 (Unit 180), respectively. A date of 2178 ± 23 RCYBP (PRI-5363) returned on oak (*Quercus*) charcoal from Sample 2 (Unit 150) represents deposition that occurred within the calibrated age range of 2310–2120 CAL yr. BP. Small and vitrified unidentifiable charcoal fragments recovered in Samples 3 (Unit 180) and 1 (Unit 200) yielded dates of 1662 ± 29 RCYBP (PRI-5535) and 399 ± 27 RCYBP (PRI-5534), respectively.

TABLE 1
PROVENIENCE DATA FOR SAMPLES FROM THE NORTH TRENCH,
SPRING VALLEY PALEOSEISMIC INVESTIGATION, SONOMA COUNTY, CALIFORNIA

Sample No.	PRI No. (AMS)	Unit	Horizontal Position	Vertical Position (mad)	Depth (mbs)	Provenience/ Description	Analysis
1	5534	200	Station 26.5	3.0	0.58	Bulk sediment	Float/Charcoal ID AMS ^{14}C Date
2	5363	150	Station 29.1	2.2	0.79	Bulk sediment	Float/Charcoal ID AMS ^{14}C Date
4	5537	400	Station 25	3	0.81	Bulk sediment	Float/Charcoal ID Microcharcoal AMS ^{14}C Date
3	5535	180	Station 27.5	2.5	1.14	Bulk sediment	Float/Charcoal ID AMS ^{14}C Date
5	5364		Station 27.5	2.1	1.14	Bulk sediment	Float/Charcoal ID Microcharcoal AMS ^{14}C Date
6	5536	160	Station 30.2	1.5	1.19	Bulk sediment	Float/Charcoal ID Microcharcoal AMS ^{14}C Date

TABLE 2
MACROFLORAL REMAINS FROM THE NORTH TRENCH,
SPRING VALLEY PALEOSEISMIC INVESTIGATION, SONOMA COUNTY, CALIFORNIA

Sample No.	Identification	Part	Charred W	Charred F	Uncharred W	Uncharred F	Weights/ Comments
1	Liters Floated						2.00 L
Unit 200	Light Fraction Weight						2.818 g
0.58 mbs	FLORAL REMAINS:						
	Roots					X	Few
	Rootlets					X	Numerous
	Sclerotia				X	X	Few
	CHARCOAL/WOOD:						
	Total charcoal ≥ 0.25 mm						0.0022 g
	Unidentifiable - small, vitrified**	Charcoal		30			0.0022 g
	NON-FLORAL REMAINS:						
	Rock					X	Few
2	Liters Floated						4.00 L
Unit 150	Light Fraction Weight						1.332 g
0.79 mbs	FLORAL REMAINS:						
	Erodium/Poaceae	Awn		1			0.0001 g
	Monocot/Herbaceous dicot	Stem		1			0.0002 g
	Parenchymous tissue			1			0.0005 g
	Vitrified tissue			4			0.0008 g
	Calandrinia	Seed			1	2	
	Caryophyllaceae	Seed				1	
	Rootlets					X	Numerous
	CHARCOAL/WOOD:						
	Total charcoal ≥ 1 mm						0.0041 g
	Quercus **	Charcoal		1			0.0039 g
	Unidentified hardwood - small	Charcoal		2			0.0002 g
	NON-FLORAL REMAINS:						
	Rock					X	Moderate

TABLE 2 (Continued)

Sample No.	Identification	Part	Charred W	Charred F	Uncharred W	Uncharred F	Weights/ Comments
4	Liters Floated						2.00 L
Unit 400	Light Fraction Weight						0.747 g
0.81 mbs	FLORAL REMAINS:						
	Rootlets					X	Numerous
	Sclerotia				X	X	Few
	CHARCOAL/WOOD:						
	Total charcoal ≥ 0.25 mm						0.0003 g
	Conifer - compressed	Charcoal		2 ic			0.0002 g
	Unidentifiable - small, vitrified	Charcoal		4			0.0001 g
	NON-FLORAL REMAINS:						
	Rock					X	Few
3	Liters Floated						1.50 L
Unit 180	Light Fraction Weight						1.489 g
1.14 mbs	FLORAL REMAINS:						
	Rootlets					X	Numerous
	CHARCOAL/WOOD:						
	Total charcoal ≥ 0.25 mm						0.0012 g
	Unidentifiable - small, vitrified**	Charcoal		14			0.0012 g
	NON-FLORAL REMAINS:						
	Rock					X	Few
5	Liters Floated						1.60 L
Unit 180	Light Fraction Weight						0.327 g
1.14 mbs	FLORAL REMAINS:						
	Rootlets					X	Numerous
	CHARCOAL/WOOD:						
	Total charcoal ≥ 0.25 mm						0.0007 g
	Unidentifiable - small, vitrified	Charcoal		18			0.0007 g
	NON-FLORAL REMAINS:						
	Rock					X	Few

TABLE 2 (Continued)

Sample No.	Identification	Part	Charred		Uncharred		Weights/ Comments
			W	F	W	F	
6	Liters Floated						0.90 L
Unit 160	Light Fraction Weight						0.161 g
1.19 mbs	FLORAL REMAINS:						
	Rootlets					X	Numerous
	CHARCOAL/WOOD:						
	Total charcoal ≥ 0.25 mm						< 0.0001 g
	Unidentifiable - small, vitrified	Charcoal		11			< 0.0001 g
	NON-FLORAL REMAINS:						
	Rock					X	Few

W = Whole
F = Fragment
X = Presence noted in sample
L = Liter
g = grams
mm = millimeters
ic = incompletely charred
**= Submitted for AMS ^{14}C Dating

TABLE 3
INDEX OF MACROFLORAL REMAINS RECOVERED FROM THE NORTH TRENCH,
SPRING VALLEY PALEOSEISMIC INVESTIGATION, SONOMA COUNTY, CALIFORNIA

Scientific Name	Common Name
FLORAL REMAINS:	
Calandrinia	Calandrinia, Red maids
Caryophyllaceae	Pink family
Erodium	Storksbill, Filaree
Monocot/Herbaceous dicot	A member of the Monocotyledonae class of Angiosperms, which include grasses, sedges, members of the agave family, lilies, and palms/ A non-woody member of the Dicotyledonae class of Angiosperms
Poaceae	Grass family
Parenchymous tissue	Relatively undifferentiated tissue composed of many similar cells with thin primary walls–occurs in different plant organs in varying amounts, especially large fleshy organs such as roots and stems, but also fruits, seeds, cones, periderm (bark), leaves, needles, etc.
Vitrified tissue	Charred material with a shiny, glassy appearance due to fusion by heat
Sclerotia	Resting structures of mycorrhizae fungi
CHARCOAL/WOOD:	
Conifer	Cone-bearing, gymnospermous trees and shrubs, mostly evergreens, including the pine, spruce, fir, juniper, cedar, yew, hemlock, redwood, and cypress
Quercus	Oak
Unidentified hardwood - small	Wood from a broad-leaved flowering tree or shrub, fragments too small for further identification
Unidentifiable - small	Charcoal fragments too small for further identification
Unidentifiable - vitrified	Charcoal exhibiting a shiny, glassy appearance due to fusion by heat

TABLE 4
RADIOCARBON RESULTS FOR SAMPLES FROM THE NORTH TRENCH,
SPRING VALLEY PALEOSEISMIC INVESTIGATION, SONOMA COUNTY, CALIFORNIA

PRI AMS No. & Sample No.	Sample Identification	AMS ^{14}C Date*	1-sigma Calibrated Date (68.2%)	2-sigma Calibrated Date (95.4%)	δ^{13}C ($^{o}/_{oo}$)
PRI-5534 1	Unidentifiable charcoal, vitrified	399 ± 27 RCYBP	510–460; 350–340 CAL yr. BP	520–420; 380–320 CAL yr. BP	-26.33
PRI-5363 2	*Quercus* charcoal	2178 ± 23 RCYBP	2310–2240; 2180–2170; 2160–2140 CAL yr. BP	2310–2220; 2210–2120 CAL yr. BP	-25.8
PRI-5537 4	Microcharcoal	6115 ± 25 RCYBP	7150–7120; 7010–6940 CAL yr. BP	7160–7050; 7030–6890 CAL yr. BP	-26.35
PRI-5535 3	Unidentifiable charcoal, vitrified	1662 ± 29 RCYBP	1610–1530 CAL yr. BP	1690–1670; 1630–1520; 1460–1440; 1430–1420 CAL yr. BP	-25.72
PRI-5364 5	Microcharcoal	2830 ± 24 RCYBP	2970–2880 CAL yr. BP	3000–2860 CAL yr. BP	-27.88
PRI-5536 6	Microcharcoal	4192 ± 24 RCYBP	4830–4810; 4760–4700; 4670–4650 CAL yr. BP	4840–4790; 4770–4620 CAL yr. BP	-27.43

* Reported in radiocarbon years at 1 standard deviation measurement precision (68.2%), corrected for δ^{13}C.

PaleoResearch Institute
2675 Youngfield Street, Golden, CO 80401
(303) 277-9848 • Fax (303) 462-2700
www.paleoresearch.com

FIGURE 1. PRI-5536 (6) CALIBRATION BP.

Laboratory Number (Sample Number): PRI-5536 (6)
Sample Identification: Microcharcoal
Conventional AMS ^{14}C Date: 4192 ± 24 RCYBP
1-sigma Calibrated Age Range (68.2%): 4830–4810; 4760–4700; 4670–4650 CAL yr. BP
2-sigma Calibrated Age Range (95.4%): 4840–4790; 4770–4620 CAL yr. BP
$\delta^{13}C$ ($^{o}/_{oo}$): -27.43

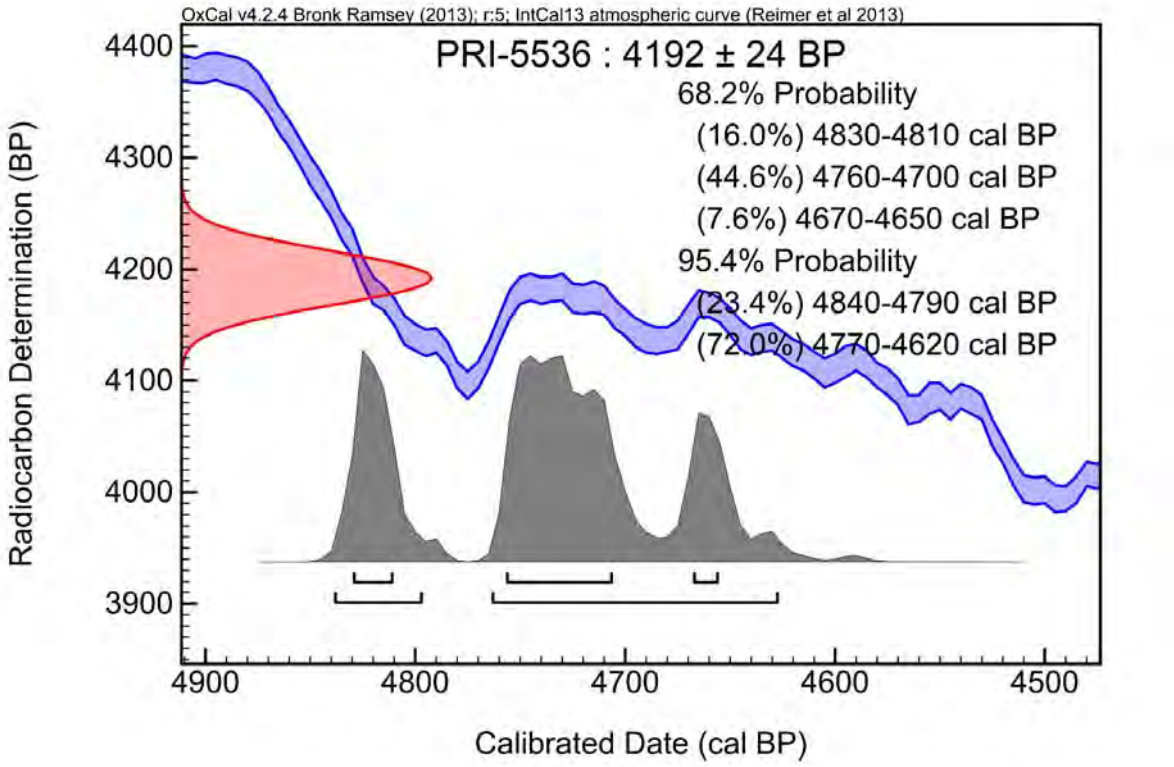

Intercept Statement. For radiocarbon calibration, PRI uses OxCal4.2.4 (Bronk Ramsey 2009; Bronk Ramsey and Lee 2013), which is a probability-based method for converting ages in radiocarbon years (RCYBP) into calibrated dates (CAL yr BP). This method is preferred over the intercept-based alternative because instead of providing individual point estimates, it reflects the probability of the date's occurrence within a given range (reflected by the amplitude [height] of the curve). As a result, the probability-based method produces more stable calibrated values than do intercept-based methods (Telford 2004). Ongoing refinements and adjustments to the calibration curve have a greater apparent effect on individual points than on ranges.

References

Bronk Ramsey, C., 2009. Bayesian analysis of radiocarbon dates. *Radiocarbon* 51(1):337-360.

Bronk Ramsey, C. and S. Lee, 2013. Recent and planned developments of the program OxCal. *Radiocarbon* 55(2-3):720–730.

Reimer, P. J., M., E. Bard, A. Bayliss, J. W. Beck, P.G. Blackwell, C. Bronk Ramsey, C. E. Buck, H. Cheng, R. L. Edwards, M. Friedrich, P. M. Grootes, T. P. Guilderson, H. Haflidason, I. Hajdas, C. Hattac, T. J. Heaton, A. G. Hogg, K. A. Hughen, K. F. Kaiser, B. Kromer, S. W. Manning, M. Niu, R. W. Reimer, D. A. Richards, E. M. Scott, J. R. Southon, C. S. M. Turney, J. van der Plicht, 2013. IntCal13 and Marine13 radiocarbon age calibration curves, 0-50,000 years cal BP. *Radiocarbon* 55(4):1869-1887.

Telford, R. J., E. Heegaard, and H. J. B. Birks, 2004. The intercept is a poor estimate of a calibrated radiocarbon age. *The Holocene* 14(2):296-298.

PaleoResearch Institute
2675 Youngfield Street, Golden, CO 80401
(303) 277-9848 • Fax (303) 462-2700
www.paleoresearch.com

FIGURE 2. PRI-5364 (5) CALIBRATION BP.

Laboratory Number (Sample Number): PRI-5364 (5)
Sample Identification: Microcharcoal
Conventional AMS ^{14}C Date: 2830 ± 24 RCYBP
1-sigma Calibrated Age Range (68.2%): 2970–2880 CAL yr. BP
2-sigma Calibrated Age Range (95.4%): 3000–2860 CAL yr. BP
$\delta^{13}C$ ($^{o}/_{oo}$): -27.88

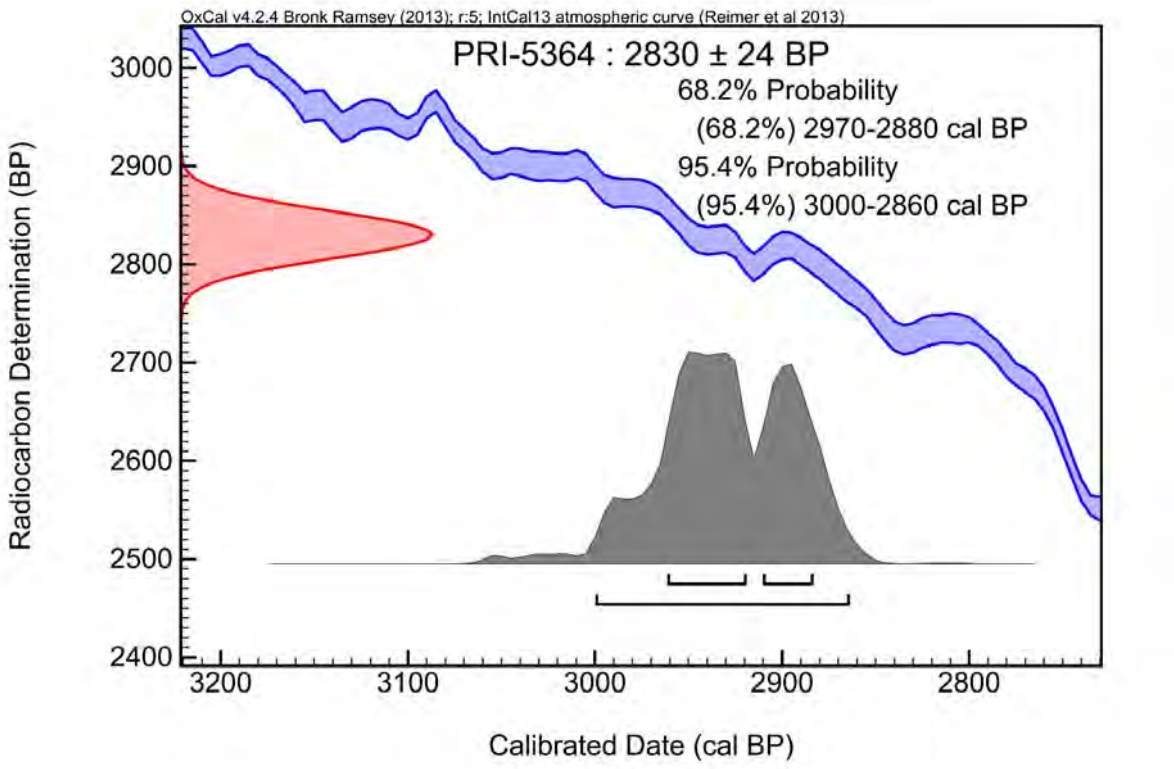

Intercept Statement. For radiocarbon calibration, PRI uses OxCal4.2.4 (Bronk Ramsey 2009; Bronk Ramsey and Lee 2013), which is a probability-based method for converting ages in radiocarbon years (RCYBP) into calibrated dates (CAL yr BP). This method is preferred over the intercept-based alternative because instead of providing individual point estimates, it reflects the probability of the date's occurrence within a given range (reflected by the amplitude [height] of the curve). As a result, the probability-based method produces more stable calibrated values than do intercept-based methods (Telford 2004). Ongoing refinements and adjustments to the calibration curve have a greater apparent effect on individual points than on ranges.

References

Bronk Ramsey, C., 2009. Bayesian analysis of radiocarbon dates. *Radiocarbon* 51(1):337-360.

Bronk Ramsey, C. and S. Lee, 2013. Recent and planned developments of the program OxCal. *Radiocarbon* 55(2-3):720–730.

Reimer, P. J., M., E. Bard, A. Bayliss, J. W. Beck, P.G. Blackwell, C. Bronk Ramsey, C. E. Buck, H. Cheng, R. L. Edwards, M. Friedrich, P. M. Grootes, T. P. Guilderson, H. Haflidason, I. Hajdas, C. Hattac, T. J. Heaton, A. G. Hogg, K. A. Hughen, K. F. Kaiser, B. Kromer, S. W. Manning, M. Niu, R. W. Reimer, D. A. Richards, E. M. Scott, J. R. Southon, C. S. M. Turney, J. van der Plicht, 2013. IntCal13 and Marine13 radiocarbon age calibration curves, 0-50,000 years cal BP. *Radiocarbon* 55(4):1869-1887.

Telford, R. J., E. Heegaard, and H. J. B. Birks, 2004. The intercept is a poor estimate of a calibrated radiocarbon age. *The Holocene* 14(2):296-298.

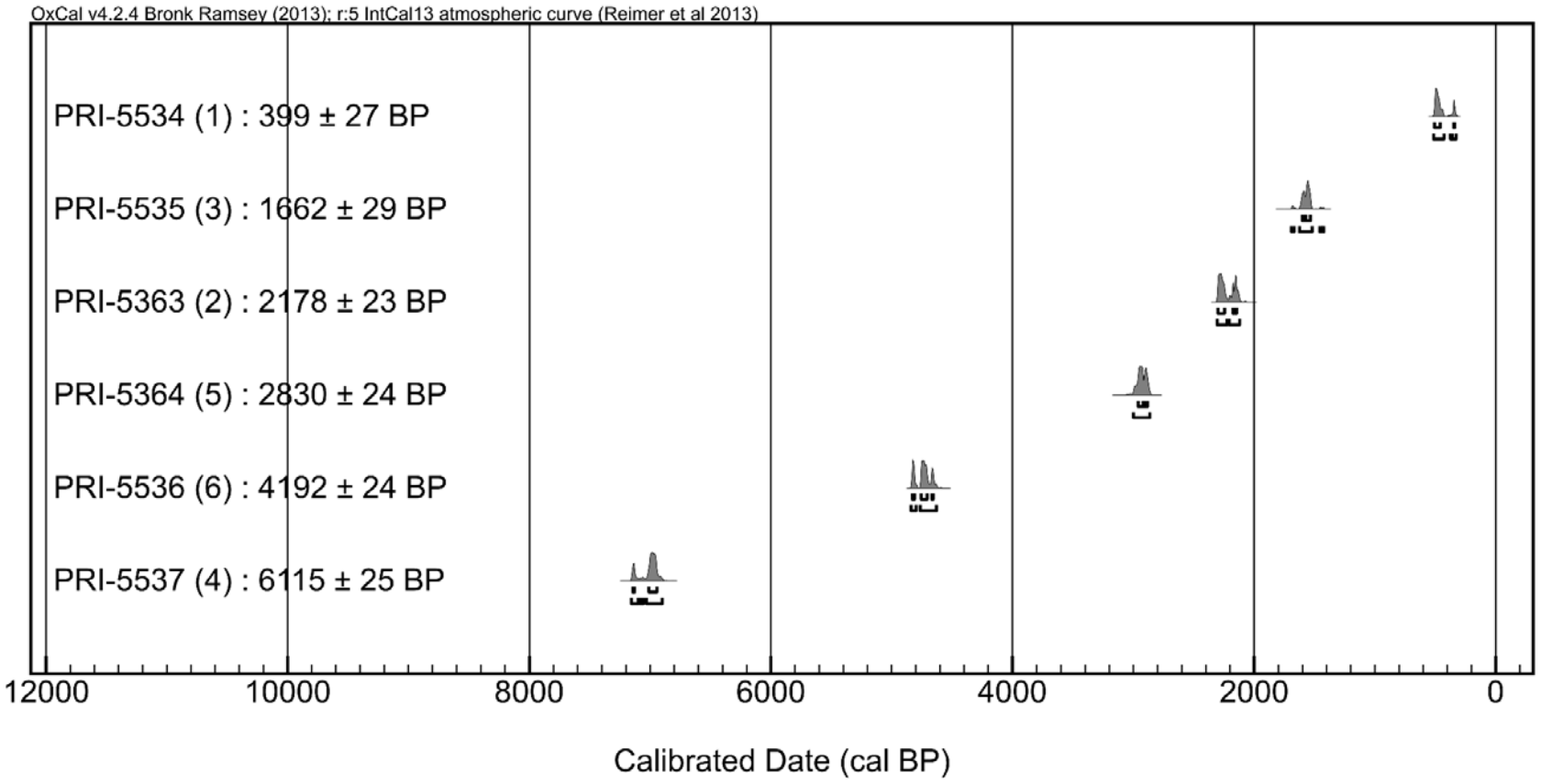

FIGURE 3. MULTIPLOT OF AMS RESULTS FOR SAMPLES FROM THE NORTH TRENCH, SPRING VALLEY PALEOSEISMIC INVESTIGATION, SAN DIEGO COUNTY, CALIFORNIA.

PaleoResearch Institute
2675 Youngfield Street, Golden, CO 80401
(303) 277-9848 • Fax (303) 462-2700
www.paleoresearch.com

FIGURE 4. PRI-5535 (3) CALIBRATION BP.

Laboratory Number (Sample Number): PRI-5535 (3)
Sample Identification: Unidentifiable charcoal, vitrified
Conventional AMS ^{14}C Date: 1662 ± 29 RCYBP
1-sigma Calibrated Age Range (68.2%): 1610–1530 CAL yr. BP
2-sigma Calibrated Age Range (95.4%): 1690–1670; 1630–1520; 1460–1440; 1430–1420 CAL yr. BP
$\delta^{13}C$ ($^{o}/_{oo}$): -25.72

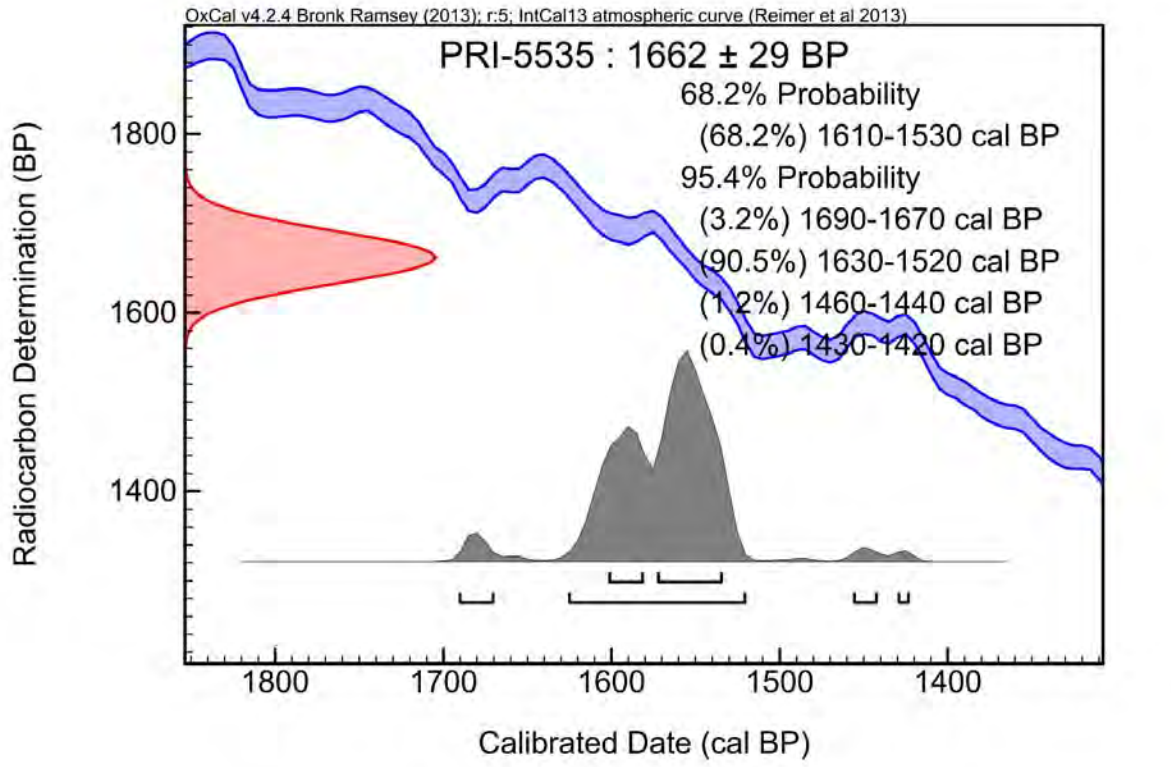

Intercept Statement. For radiocarbon calibration, PRI uses OxCal4.2.4 (Bronk Ramsey 2009; Bronk Ramsey and Lee 2013), which is a probability-based method for converting ages in radiocarbon years (RCYBP) into calibrated dates (CAL yr BP). This method is preferred over the intercept-based alternative because instead of providing individual point estimates, it reflects the probability of the date's occurrence within a given range (reflected by the amplitude [height] of the curve). As a result, the probability-based method produces more stable calibrated values than do intercept-based methods (Telford 2004). Ongoing refinements and adjustments to the calibration curve have a greater apparent effect on individual points than on ranges.

References

Bronk Ramsey, C., 2009. Bayesian analysis of radiocarbon dates. *Radiocarbon* 51(1):337-360.

Bronk Ramsey, C. and S. Lee, 2013. Recent and planned developments of the program OxCal. *Radiocarbon* 55(2-3):720–730.

Reimer, P. J., M., E. Bard, A. Bayliss, J. W. Beck, P.G. Blackwell, C. Bronk Ramsey, C. E. Buck, H. Cheng, R. L. Edwards, M. Friedrich, P. M. Grootes, T. P. Guilderson, H. Haflidason, I. Hajdas, C. Hattac, T. J. Heaton, A. G. Hogg, K. A. Hughen, K. F. Kaiser, B. Kromer, S. W. Manning, M. Niu, R. W. Reimer, D. A. Richards, E. M. Scott, J. R. Southon, C. S. M. Turney, J. van der Plicht, 2013. IntCal13 and Marine13 radiocarbon age calibration curves, 0-50,000 years cal BP. *Radiocarbon* 55(4):1869-1887.

Telford, R. J., E. Heegaard, and H. J. B. Birks, 2004. The intercept is a poor estimate of a calibrated radiocarbon age. *The Holocene* 14(2):296-298.

PaleoResearch Institute
2675 Youngfield Street, Golden, CO 80401
(303) 277-9848 • Fax (303) 462-2700
www.paleoresearch.com

FIGURE 5. PRI-5537 (4) CALIBRATION BP.

Laboratory Number (Sample Number): PRI-5537 (4)
Sample Identification: Microcharcoal
Conventional AMS ^{14}C Date: 6115 ± 25 RCYBP
1-sigma Calibrated Age Range (68.2%): 7150–7120; 7010–6940 CAL yr. BP
2-sigma Calibrated Age Range (95.4%): 7160–7050; 7030–6890 CAL yr. BP
$\delta^{13}C$ ($^{o}/_{oo}$): -26.35

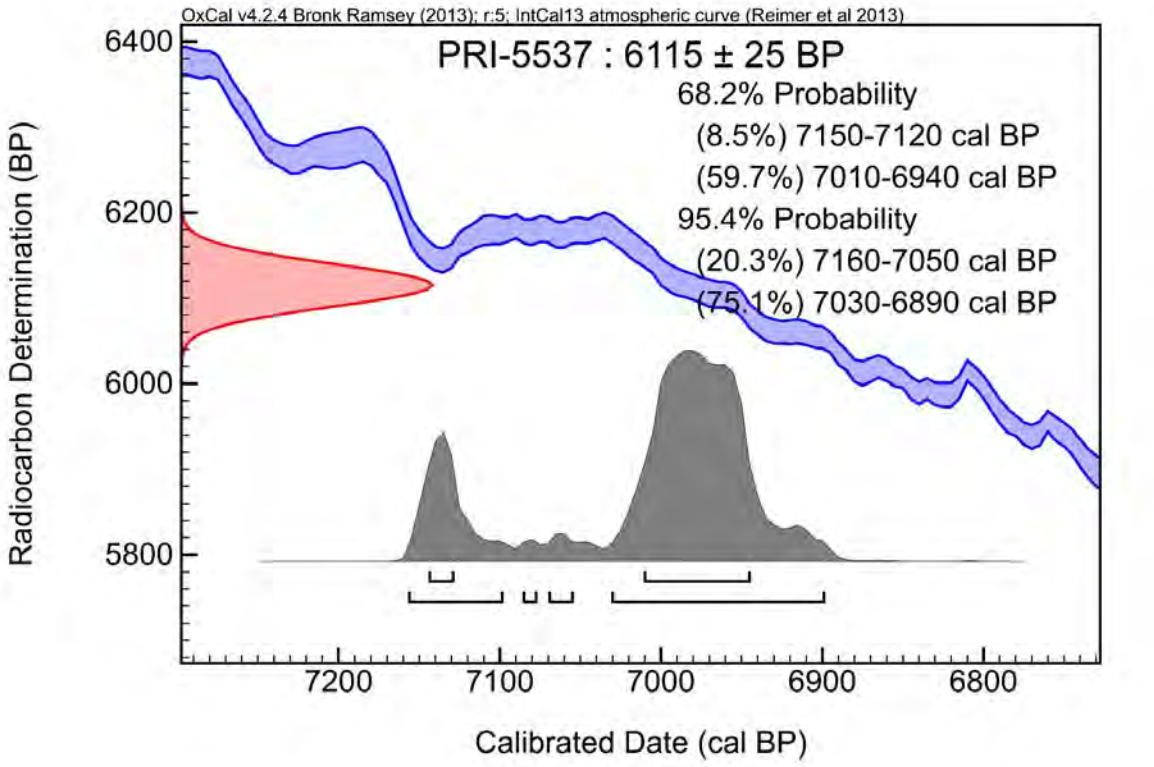

Intercept Statement. For radiocarbon calibration, PRI uses OxCal4.2.4 (Bronk Ramsey 2009; Bronk Ramsey and Lee 2013), which is a probability-based method for converting ages in radiocarbon years (RCYBP) into calibrated dates (CAL yr BP). This method is preferred over the intercept-based alternative because instead of providing individual point estimates, it reflects the probability of the date's occurrence within a given range (reflected by the amplitude [height] of the curve). As a result, the probability-based method produces more stable calibrated values than do intercept-based methods (Telford 2004). Ongoing refinements and adjustments to the calibration curve have a greater apparent effect on individual points than on ranges.

References

Bronk Ramsey, C., 2009. Bayesian analysis of radiocarbon dates. *Radiocarbon* 51(1):337-360.

Bronk Ramsey, C. and S. Lee, 2013. Recent and planned developments of the program OxCal. *Radiocarbon* 55(2-3):720–730.

Reimer, P. J., M., E. Bard, A. Bayliss, J. W. Beck, P.G. Blackwell, C. Bronk Ramsey, C. E. Buck, H. Cheng, R. L. Edwards, M. Friedrich, P. M. Grootes, T. P. Guilderson, H. Haflidason, I. Hajdas, C. Hattac, T. J. Heaton, A. G. Hogg, K. A. Hughen, K. F. Kaiser, B. Kromer, S. W. Manning, M. Niu, R. W. Reimer, D. A. Richards, E. M. Scott, J. R. Southon, C. S. M. Turney, J. van der Plicht, 2013. IntCal13 and Marine13 radiocarbon age calibration curves, 0-50,000 years cal BP. *Radiocarbon* 55(4):1869-1887.

Telford, R. J., E. Heegaard, and H. J. B. Birks, 2004. The intercept is a poor estimate of a calibrated radiocarbon age. *The Holocene* 14(2):296-298.

FIGURE 6. PRI-5363 (2) CALIBRATION BP.

Laboratory Number (Sample Number): PRI-5363 (2)
Sample Identification: *Quercus* charcoal
Average Lifespan: Variable, depending on species, from 100–400+ years
Conventional AMS ^{14}C Date: 2178 ± 23 RCYBP
1-sigma Calibrated Age Range (68.2%): 2310–2240; 2180–2170; 2160–2140 CAL yr. BP
2-sigma Calibrated Age Range (95.4%): 2310–2220; 2210–2120 CAL yr. BP
$\delta^{13}C$ ($^{o}/_{oo}$): -25.8

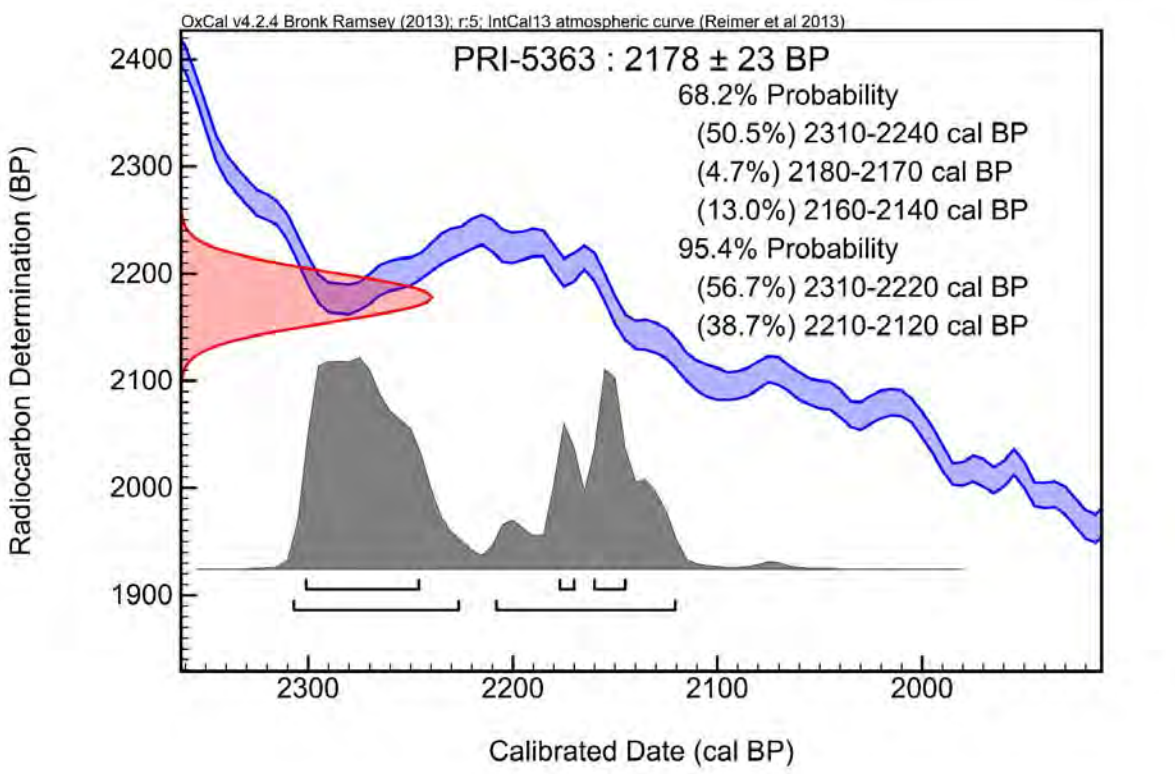

Intercept Statement. For radiocarbon calibration, PRI uses OxCal4.2.4 (Bronk Ramsey 2009; Bronk Ramsey and Lee 2013), which is a probability-based method for converting ages in radiocarbon years (RCYBP) into calibrated dates (CAL yr BP). This method is preferred over the intercept-based alternative because instead of providing individual point estimates, it reflects the probability of the date's occurrence within a given range (reflected by the amplitude [height] of the curve). As a result, the probability-based method produces more stable calibrated values than do intercept-based methods (Telford 2004). Ongoing refinements and adjustments to the calibration curve have a greater apparent effect on individual points than on ranges.

References

Bronk Ramsey, C., 2009. Bayesian analysis of radiocarbon dates. *Radiocarbon* 51(1):337-360.

Bronk Ramsey, C. and S. Lee, 2013. Recent and planned developments of the program OxCal. *Radiocarbon* 55(2-3):720–730.

Reimer, P. J., M., E. Bard, A. Bayliss, J. W. Beck, P.G. Blackwell, C. Bronk Ramsey, C. E. Buck, H. Cheng, R. L. Edwards, M. Friedrich, P. M. Grootes, T. P. Guilderson, H. Haflidason, I. Hajdas, C. Hattac, T. J. Heaton, A. G. Hogg, K. A. Hughen, K. F. Kaiser, B. Kromer, S. W. Manning, M. Niu, R. W. Reimer, D. A. Richards, E. M. Scott, J. R. Southon, C. S. M. Turney, J. van der Plicht, 2013. IntCal13 and Marine13 radiocarbon age calibration curves, 0-50,000 years cal BP. *Radiocarbon* 55(4):1869-1887.

Telford, R. J., E. Heegaard, and H. J. B. Birks, 2004. The intercept is a poor estimate of a calibrated radiocarbon age. *The Holocene* 14(2):296-298.

FIGURE 7. PRI-5534 (1) CALIBRATION BP.

Laboratory Number (Sample Number): PRI-5534 (1)
Sample Identification: Unidentifiable charcoal, vitrified
Conventional AMS ^{14}C Date: 399 ± 27 RCYBP
1-sigma Calibrated Age Range (68.2%): 510–460; 350–340 CAL yr. BP
2-sigma Calibrated Age Range (95.4%): 520–420; 380–320 CAL yr. BP
$\delta^{13}C$ ($^{o}/_{oo}$): -26.33

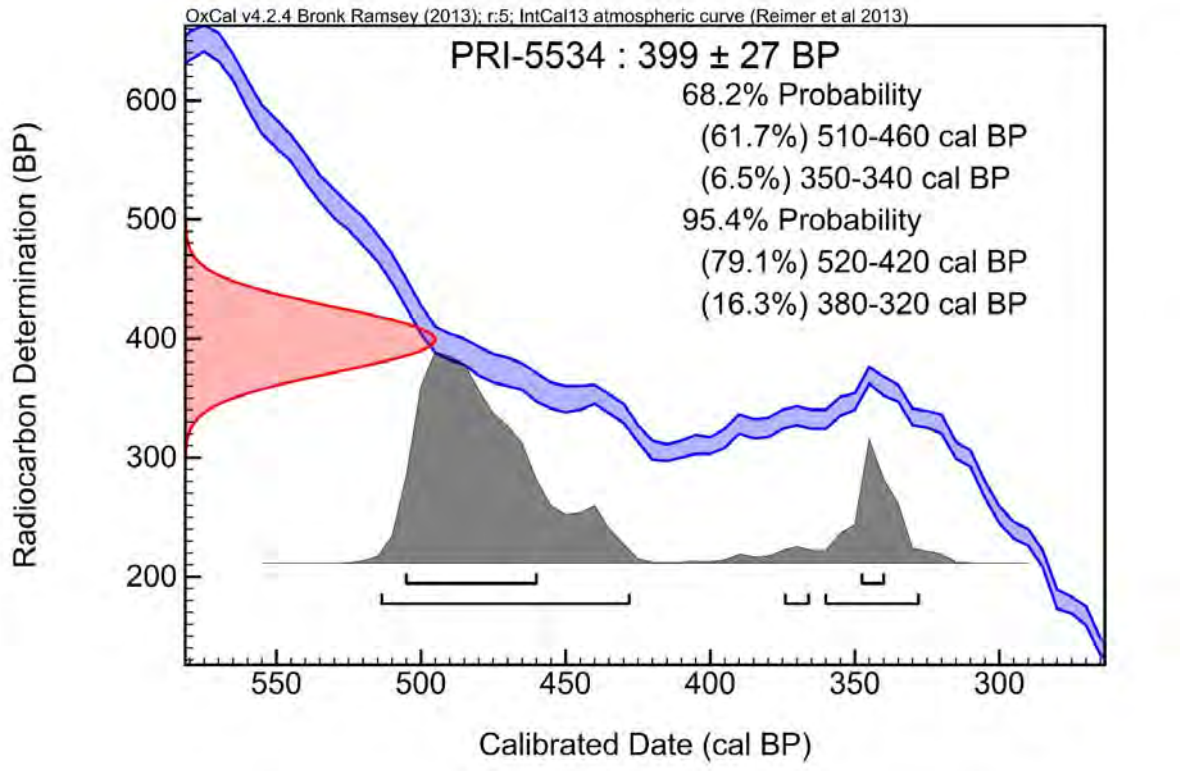

Intercept Statement. For radiocarbon calibration, PRI uses OxCal4.2.4 (Bronk Ramsey 2009; Bronk Ramsey and Lee 2013), which is a probability-based method for converting ages in radiocarbon years (RCYBP) into calibrated dates (CAL yr BP). This method is preferred over the intercept-based alternative because instead of providing individual point estimates, it reflects the probability of the date's occurrence within a given range (reflected by the amplitude [height] of the curve). As a result, the probability-based method produces more stable calibrated values than do intercept-based methods (Telford 2004). Ongoing refinements and adjustments to the calibration curve have a greater apparent effect on individual points than on ranges.

References

Bronk Ramsey, C., 2009. Bayesian analysis of radiocarbon dates. *Radiocarbon* 51(1):337-360.

Bronk Ramsey, C. and S. Lee, 2013. Recent and planned developments of the program OxCal. *Radiocarbon* 55(2-3):720–730.

Reimer, P. J., M., E. Bard, A. Bayliss, J. W. Beck, P.G. Blackwell, C. Bronk Ramsey, C. E. Buck, H. Cheng, R. L. Edwards, M. Friedrich, P. M. Grootes, T. P. Guilderson, H. Haflidason, I. Hajdas, C. Hattac, T. J. Heaton, A. G. Hogg, K. A. Hughen, K. F. Kaiser, B. Kromer, S. W. Manning, M. Niu, R. W. Reimer, D. A. Richards, E. M. Scott, J. R. Southon, C. S. M. Turney, J. van der Plicht, 2013. IntCal13 and Marine13 radiocarbon age calibration curves, 0-50,000 years cal BP. *Radiocarbon* 55(4):1869-1887.

Telford, R. J., E. Heegaard, and H. J. B. Birks, 2004. The intercept is a poor estimate of a calibrated radiocarbon age. *The Holocene* 14(2):296-298.

REFERENCES CITED

Berger, R.
1970 The Potential and Limitations of Radiocarbon Dating in the Middle Ages: The Radiochronologist's View. In *Scientific Methods in Medieval Archaeology*, edited by R. Berger, pp. 89-139. University of California Press, Berkeley.

1972 Tree-ring Calibration of Radiocarbon Dates. In *Proceedings of the Eighth International Radiocarbon Dating Conference*, pp. A97-A103. vol. 14, T. Grant-Taylor Rafter Ra, general editor. Royal Society of New Zealand, Wellington.

Bronk Ramsey, C., and S. Lee
2013 Recent and Planned Developments of the Program OxCal. *Radiocarbon* 55(2-3):720-730.

Bronk Ramsey, Christopher
2009 Bayesian Analysis of Radiocarbon Dates. *Radiocarbon* 51(1):337-360.

Carlquist, Sherwin
2001 *Comparative Wood Anatomy: Systematic, Ecological, and Evolutionary Aspects of Dicotyledon Wood*. 2nd ed. Springer Series in Wood Science. Springer, Berlin.

Gulliksen, S., and E. M. Scott
1995 Report of the TIRI Workshop. The 15th International Radiocarbon Conference. *Radiocarbon* 37(2):820-821.

Hather, Jon G.
2000 *Archaeological Parenchyma*. Archetype Publications Ltd., London.

Hoadley, Bruce
1990 *Identifying Wood: Accurate Results with Simple Tools*. The Taunton Press, Inc., Newtown.

Kaelin, Paul E., William W. Huggett, and Ken B. Anderson
2006 Comparison of Vitrified and Unvitrified Eocene Woody Tissues by TMAH thermochemolysis - Implications for the Early Stages of the Formation of Vitrinite. *Geochemical Transactions* 7(9):12.

Kricher, John C., and Gordon Morrison
1988 *A Field Guide to Ecology of Eastern Forests*. The Peterson Field Guide Series. Houghton Mifflin Company, Boston and New York.

Marguerie, D., and J. Y. Hunot
2007 Charcoal Analysis and Dendrology: Data from Archaeological Sites in Northwestern France. *Journal of Archaeological Science* 34:1417-1433.

Martin, Alexander C., and William D. Barkley
1961 *Seed Identification Manual*. University of California, Berkeley.

Matthews, Meredith H.
1979 Soil Sample Analysis of 5MT2148: Dominguez Ruin, Dolores, Colorado. Appendix B. In *The Dominguez Ruin: A McElmo Phase Pueblo in Southwestern Colorado*, edited by Alan D. Reed. Cultural Resource Series No. 7. Bureau of Land Management, Denver.

Mauseth, James D.
1988 Parenchyma. Chapter 3. In *Plant Anatomy*, pp. 43-51. The Benjamin/Cummings Publishing Company, Inc., Menlo Park, California.

Mcparland, Laura C., Margaret E. Collinson, Andrew C. Scott, Gill Campbell, and Robyn Veal
2010 Is Vitrification in Charcoal a Result of High Temperature Burning of Wood? *Journal of Archaeological Science* 37:2679-2687.

Mcweeney, Lucinda
1989 What Lies Lurking Below the Soil: Beyond the Archaeobotanical View of Flotation Samples. *North American Archaeologist* 10(3):227-230.

Musil, Albina F.
1963 *Identification of Crop and Weed Seeds*. Agricultural Handbook no. 219. U.S. Department of Agriculture, Washington, D.C.

Puseman, Kathryn
2007 Examination of Bulk Sediment, Wood Identification, and AMS Radiocarbon Analysis of Material from along the Skokomish River, Washington. Ms. on file with the Bureau of Reclamation, Denver, Colorado. PRI Technical Report 05-95/06-68.

Puseman, Kathryn, Linda Scott Cummings, and R. A. Varney
2009 Why Not Grab That Big, Juicy, Piece of Charcoal for Dating? Paper presented at the Ohio Archaeological Conference, Newark, Ohio, October 31-November 1, 2009.

Reimer, P. J., E. Bard, A. Bayliss, J. W. Beck, P. G. Blackwell, C. B. Ramsey, C. E. Buck, H. Cheng, R. L. Edwards, M. Friedrich, P. M. Grootes, T. P. Guilderson, H. Haflidason, I. Hajdas, C. Hatte, T. J. Heaton, D. L. Hoffmann, A. G. Hogg, K. A. Hughen, K. F. Kaiser, B. Kromer, S. W. Manning, M. Niu, R. W. Reimer, D. A. Richards, E. M. Scott, J. R. Southon, R. A. Staff, C. S. M. Turney, and J. Van Der Plicht
2013 InterCal 13 and Marine 13 Radiocarbon Age Calibration Curves 0-50,000 Years Cal BP. *Radiocarbon* 55(4):1869-1887.

Rutherford, David W., Robert L. Wershaw, and Larry G. Cox
2005 *Changes in Composition and Porosity Occurring During the Thermal Degradation of Wood and Wood Components*. 2004-5292. Copies available from U.S. Department of the Interior, U.S. Geological Survey.

Schopmeyer, C. S.
1974 *Seeds of Woody Plants in the United States*. Agricultural Handbook No. 450. United States Department of Agriculture, Washington, D.C.

Schweingruber, Fritz Hans, Annett Borner, and Ernst-Detlef Schulze
2011 *Atlas of Stem Anatomy in Herbs, Shrubs and Trees* Vol I. Springer-Verlag, Berlin Heidelberg.

2013 *Atlas of Stem Anatomy in Herbs, Shrubs and Trees* Vol. II. Springer-Verlag, Berlin Heidelberg.

Taylor, R. E.
1987 *Radiocarbon Dating: An Archaeological Perspective*. Academic Press, Inc., Orlando.

Taylor, R. E., and Ofer Bar-Yosef (editors)
2014 *Radiocarbon Dating: An Archaeological Perspective*. 2nd ed. Left Coast Press, Inc., Walnut Creek.

Telford, Richard J., E. Heegaard, and H. J. B. Birks
2004 The Intercept is a Poor Estimate of a Calibrated Radiocarbon Age. *The Holocene* 14(2):296-298.

Trappe, James M.
1962 Fungus Associates of Ectotrophic Mycorrhizae. In *The Botanical Review*. U.S. Department of Agriculture, Washington, D.C.